Novel roles for phospholipase C in plant stress signalling and development

Zhang, Q.

Publication date
2017
Document Version
Other version
License
Other

Chapter 2

A role for Arabidopsis phospholipase C3 (*PLC3*) in seed germination, lateral root formation and stomatal closure

Qianqian Zhang,[1,2] Ringo van Wijk,[1,2] Muhammad Shahbaz,[1#] Wendy Roels,[1] Bas van Schooten,[1] Joop E.M. Vermeer,[1,3] Aisha Guardia, [4] Denise Scuffi, [4] Carlos García-Mata,[4] Debabrata Laha,[5] Phoebe Williams,[6] Leo A.J. Willems,[7] Wilco Ligterink,[7] Susanne Hoffmann-Benning,[8] Glenda Gillaspy,[6] Gabriel Schaaf,[5] Michel A. Haring,[1] Ana M. Laxalt,[4] & Teun Munnik[1,2]

[1]Section Plant Physiology or [2]Section Plant Cell Biology, Swammerdam Institute for Life Sciences, University of Amsterdam, Science Park 904, Amsterdam, 1098 XH, The Netherlands, [3]Dept. of Plant and Microbial Biology, University of Zürich, Zürich, Switzerland, [4]Instituto de Investigaciones Biológicas (IIB-CONICET-UNMdP), Universidad Nacional de Mar del Plata, Mar del Plata, Argentina, [5]Center for Plant Molecular Biology, University of Tübingen, Tübingen, Germany, [6]Dept. of Biochemistry, Virginia Polytechnic Institute and State University, Blacksburg, VA, USA, [7]Lab. of Plant Physiology, Wageningen University, Droevendaalsesteeg 1, 6708 PB, Wageningen, The Netherlands, and [8]Dept. of Biochemistry & Molecular Biology, Michigan State University, East Lansing, MI, USA, [#]Current address: Dept. of Botany, University of Agriculture, Faisalabad, Pakistan.

ABSTRACT

Phospholipase C (PLC) is best known for its role in generating second messengers by hydrolysis of phosphatidylinositol 4,5-bisphosphate (PIP_2) in mammalian cells. In plants however, PLC's role is less clear as plants lack the prime targets for both inositol 1,4,5-trisphosphate (i.e. a ligand-gated Ca^{2+} channel) and diacylglycerol (i.e. protein kinase C and TRP-type ion channels). The genome of *Arabidopsis thaliana* encodes for 9 *PLC* genes. Here, we analyzed the role of PLC3. Promoter-GUS analyses revealed that *PLC3* is specifically expressed in the vascular tissue (most likely phloem) of roots, leaves and flowers, but also in guard cells and at the base of trichomes. Knock-out mutants of *PLC3* were found to be affected in seed germination, root development and stomatal closure. Using *in vivo* $^{32}P_i$-lipid labeling analyses, we found that ABA stimulated the formation of PIP_2 in wild type germinating seeds, seedlings and guard cell-enriched leaf peels, but not in *plc3* mutants. The latter displayed decreased sensitivity to ABA during seed-germination inhibition and ABA induced-stomatal closure. Overexpression of *PLC3* enhanced drought tolerance and decreased stomatal aperture. Together, our results uncovered novel roles for *PLC3* in ABA signaling and plant development.

Key words: PLC; seed germination; lateral root formation; stomatal closure; drought tolerance.

INTRODUCTION

Phospholipase C (PLC) is well known for its role in phospholipid signaling in animals. In this classical paradigm, extracellular receptor occupation leads to the activation of intracellular PLC, which hydrolyzes the minor lipid phosphatidylinositol 4,5-bisphosphate (PIP_2) to produce two second messengers, inositol 1,4,5- trisphosphate (IP_3) and diacylglycerol (DAG). IP_3 diffuses into the cytosol where it triggers the release of Ca^{2+} from an intracellular store via an IP_3 receptor that is a ligand-gated Ca^{2+} channel, whereas DAG remains in the plasma membrane where it recruits and activates members of the protein kinase C (PKC) family or stimulates TRP- (transient receptor potential-) ion channels. Subsequent changes in Ca^{2+} and phosphorylation status affect multiple protein targets and hence, downstream cellular processes (Irvine, 2006; Michell, 2008; Balla, 2013).

Less is clear about the PLC-signaling paradigm in plants (Munnik, 2014). Most importantly, all higher plant genomes sequenced so far, lack homologs of an IP_3 receptor, PKC or TRP channel, which are supposed to be the primary targets of this signaling system (Wheeler and Brownlee, 2008; Munnik and Testerink, 2009; Munnik and Vermeer, 2010; Munnik and Nielsen, 2011; Munnik, 2014; Heilmann, 2016). Initially, microinjected IP_3 had been shown to release Ca^{2+} from an intracellular store (Gilroy *et al*., 1990; Blatt *et al*., 1990; Allen and Sanders, 1994) indicating that plants cells exhibited a genuine IP_3 receptor (Hunt and Gray, 2001) but Brearley's lab later provided evidence that this IP_3 is phosphorylated into IP_6 within seconds, and that the latter compound is likely to be responsible for the store-operated Ca^{2+} release (Lemtiri-Chlieh *et al.*, 2000, 2003; Munnik and Vermeer, 2010). Similarly, not DAG but its phosphorylated product, phosphatidic acid (PA) is emerging as the plant lipid-second messenger (Munnik, 2001; Testerink and Munnik, 2005; Arisz *et al*., 2009; Pokotylo *et al*., 2014; Munnik, 2014; Vermeer *et al*., 2017).

Evidence that PLC is important for plants has come from various studies. Silencing of *PLC1* in Arabidopsis and tobacco has indicated a role for a PLC in ABA signaling and stomatal closure (Sanchez and Chua, 2001a; Hunt *et al*., 2003). ABA also induces the expression of some *PLC* genes (Hirayama *et al.*, 1995; Lin *et al.*, 2004; Tasma *et al.*, 2008; Pokotylo *et al.*, 2014). A link between ABA and polyphosphoinositide (PPI) turnover has been reported, but the data is quite controversial (Munnik and Vermeer, 2010). Nonetheless, ABA has been shown to trigger IP_6 responses within minutes in potato guard cell protoplasts and duck weed turions (Flores and Smart, 2000; Lemtiri-Chlieh *et al.*, 2000, 2003), and to elevate intracellular Ca^{2+} levels in a variety of plant (Lee *et al*., 1996; Staxen *et al*., 1999; Blatt, 2000; Schroeder *et al*., 2001; Munemasa *et al*., 2015; Assmann and Jegla, 2016) Whether the formation of IP_6 is PLC-dependent and related to ABA-mediated signaling is still unknown.

Apart from ABA, PLC signaling has been linked to several other abiotic stresses, including salt, drought (mimicked by sorbitol, mannitol or PEG) and heat stress. Interestingly, these stresses are also known to trigger an increase in the level of PIP_2 (Pical *et al*., 1999; DeWald *et al*., 2001; Zonia and Munnik, 2004; van Leeuwen *et al*., 2007; Darwish *et al*., 2009; Mishkind *et al*., 2009; Horvath *et al*.,

2012). In some cases, IP_3 responses were reported, but none addressed IP_6 levels or other inositolpolyphosphates (IPPs) that are emerging as signalling molecules, i.e. IP_5, IP_7 and IP_8 (Takahashi *et al.*, 2001; Huang, *et al.*, 2006; Liu, *et al.*, 2006; Zheng *et al.*, 2012; Gilaspy 2013; Laha *et al*., 2015, 2016). Decreases of PIP have also been reported (Cho *et al.*, 1993; Pical *et al.*, 1999; DeWald *et al.*, 2001; Vermeer *et al.*, 2009; Zarza *et al.*, unpublished) and theoretically, PLC could use PIP as a substrate as well. *In vitro*, both PPIs are hydrolyzed equally well and *in vivo,* there is enough PIP in the plasma membrane of plants, where PIP_2 is typically missing, and in general only present at very low concentrations (20-100x less than mammalian cells; Munnik *et al*., 1994; 1998a,b Munnik, 2014; Zarza *et al*., unpublished). Interestingly, overexpression of *PLC* in maize, canola and tobacco has been shown to increase the plant's tolerance to salinity-, drought- and/or cold stress (Wang *et al.*, 2008; Georges *et al.*, 2009; Tripathy *et al.*, 2011; Nokhrina *et al.*, 2014), although it is not yet clear how the plant achieves this (Das *et al.*, 2005; Georges *et al.*, 2009).

PLC has also been implicated in plant-microbe interactions (Laxalt and Munnik, 2002) both symbiotic and pathogenic (Luit *et al.*, 2000; Hartog *et al.*, 2003; De Jong *et al.*, 2004; Gonorazky *et al.*, 2014, 2016). Some of the pathogenic responses have been shown comprise nitric oxide (NO) signalling (Lanteri *et al.*, 2011; Raho *et al.*, 2011). Recently, Vossen *et al*. (2010) presented the first genetic evidence for PLC's contribution in tomato disease resistance (Vossen *et al.*, 2010).

Apart from stress, PLC signalling has also been connected to various growth- and developmental responses. For example, *Arabidopsis PLC2* and *Torenia fournieri PLC1* are involved in auxin modulated-reproductive development (Song *et al.*, 2008; Li *et al.*, 2015; Di Fino *et al.*, 2017), while petunia *PLC1* and tobacco *PLC3* regulate tip growth in pollen tubes (Dowd *et al.*, 2006; Helling *et al.*, 2006). In *Physcomitrella patens, PLC1* has been shown to play a role in the cytokinin- and gravity response (Repp *et al.*, 2004).

The Arabidopsis genome encodes 9 *PLC* genes (Mueller-roeber and Pical, 2002). So far, no developmental disorders other than the reproduction mentioned above have been reported for Arabidopsis KO mutants, presumably due to genetic redundancy. Here, we show that *PLC3* plays various, yet subtle roles in plant development and ABA signaling, and that overexpression increases drought tolerance.

RESULTS

Loss of *PLC3* affects root development

To investigate *PLC3* function, we isolated two homozygous T-DNA insertion mutants of *PLC3*, *plc3-2* (SALK_037453) and *plc3-3* (SALK_054406) with T-DNA inserts in exon 3 and intron 3 located in the X-domain, respectively (Fig. 1a). Reduction of *PLC3* expression was verified by both reverse transcription (RT)-PCR (Fig. 1b) and Q-PCR (Fig. 1c).

Growing seedlings on ½MS plates, a subtle difference in root system architecture between wild type and *plc3* mutants was found. Both *PLC3* deficient lines exhibited slightly shorter primary roots (~5%) and developed less (~15%) lateral roots than wild type. The mutants also showed low lateral root density (~10%) (Figs. 1d, 1e).

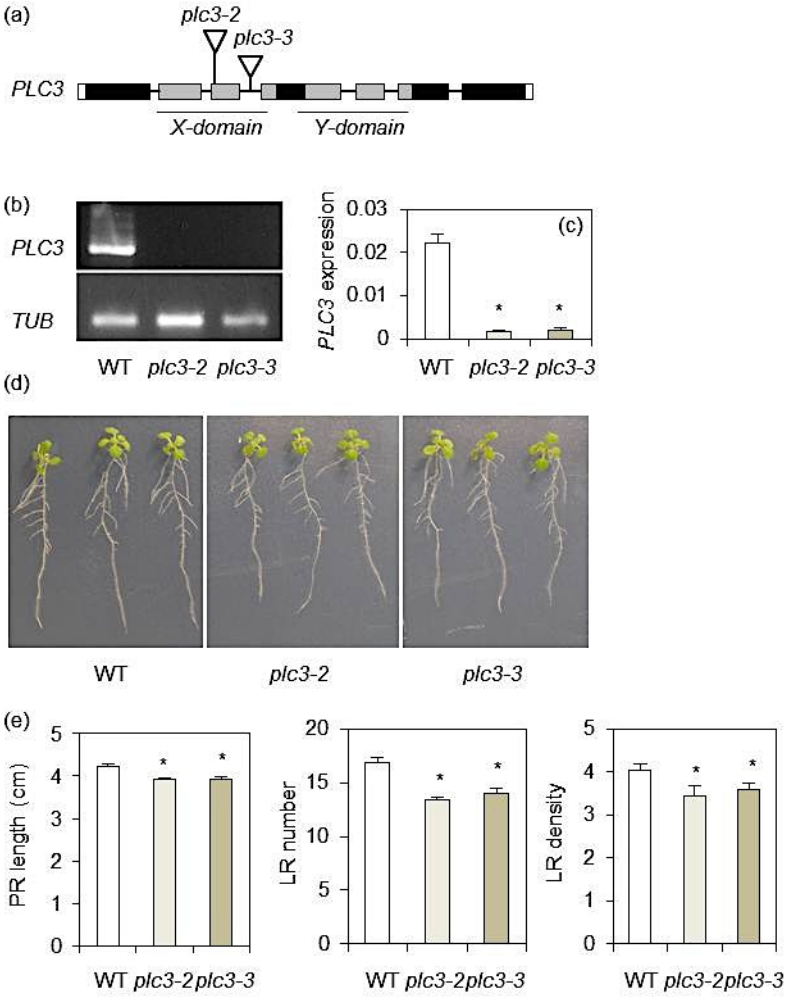

Figure 1. Effect of *PLC3* knockout on seedling root development
(a) Representation of *PLC3* gene and T-DNA insertion positions of *plc3-2* and *plc3-3*. Filled boxed and lines represent exons and introns, respectively. Open, grey boxes and triangle represent untranslated region, X- and Y- domains and T-DNA insertions, respectively. (b) Confirmation of reduction of *PLC3* expression in *plc3* lines by cDNA amplification. *PLC3*-specific primers were used to detect *PLC3* mRNA by RT-PCR. *TUBULINα4* (*TUB*) was used as loading control. (c) *PLC3* expression level in wild-type, *plc3-2* and *plc3-3* lines measured by Q-PCR. Relative expression is based on comparison to expression of the *SAND* gene. Values are means ± SD (n = 3) for one representative experiment. (d) Seedling morphology of wild-type and *plc3* mutants. Seeds were germinated on ½ MS with 0.5% sucrose for 4 days, then transferred to ½MS plates without sucrose. Photographs were taken 12 days after germination (DAG). (e) Primary root (PR) length, lateral root (LR) number and lateral root (LR) density at 12 DAG. Values are means ± SE of three independent experiments (n>20). Asterisk (*) indicate significance at P<0.05 compared to wt based on Student's *t* test.

Expression of *PLC3* during plant development

Changes in transcript level of *PLC3* in various organs and upon induction by hormones or abiotic stress have been reported using quantitative RT-PCR (Hunt *et al.*, 2004; Tasma *et al.*, 2008). To investigate this further, we generated β-glucuronidase- (GUS-) and YFP- reporter lines, driven by a *2.4 kb PLC3* promoter fragment (*PLC3*$_{pro}$*:GUS-YFP*). As shown in Figure 2, GUS activity was mainly found in the vasculature, throughout all stages of development, including seedling, cotyledons, leaves, hypocotyl, flower, incl. stamen and style, and during seed development. Interestingly, the base of the trichomes revealed GUS expression (Fig. 2j-k), which again appears to be linked to the vascular system (Fig. 2k). The expression in the main root was not homogenous. At the distal side of the root maturation zone, the GUS expression tended to be 'segmented', while in the apical maturation zone it was continuous, and expression stopped near the transition zone (Fig. 2c-i). Interestingly, lateral roots always emerged from a segment, but not every segment led to a lateral root (Fig. 2c, d). To search for a potential correlation, we analysed GUS expression in seedlings grown on a plate that was positioned in a 45º angle, which forces lateral roots to emerge at the curved sites. Under these conditions, less segments were found but all lateral roots did emerge from a segment (Supplemental Fig. S1). A similar segmented pattern was observed in tertiary root formation (Fig. 2e). Together these results confirm that PLC3 is expressed throughout the plant, but the expression is mainly restricted to the vasculature (Hunt *et al.*, 2004; Tasma *et al.*, 2008).

To obtain more detailed information about the *PLC3* expression within the vasculature, optical cross- and longitudinal sections were made by confocal microscopy (Supplemental Fig. S2). From this data, YFP expression appeared to be localized to the phloem and this correlated with data from the eFP browser, where *PLC3* seems to be predominantly expressed in the companion cells (http://www.bar.utoronto.ca/efp/cgi-bin/efpWeb.cgi).

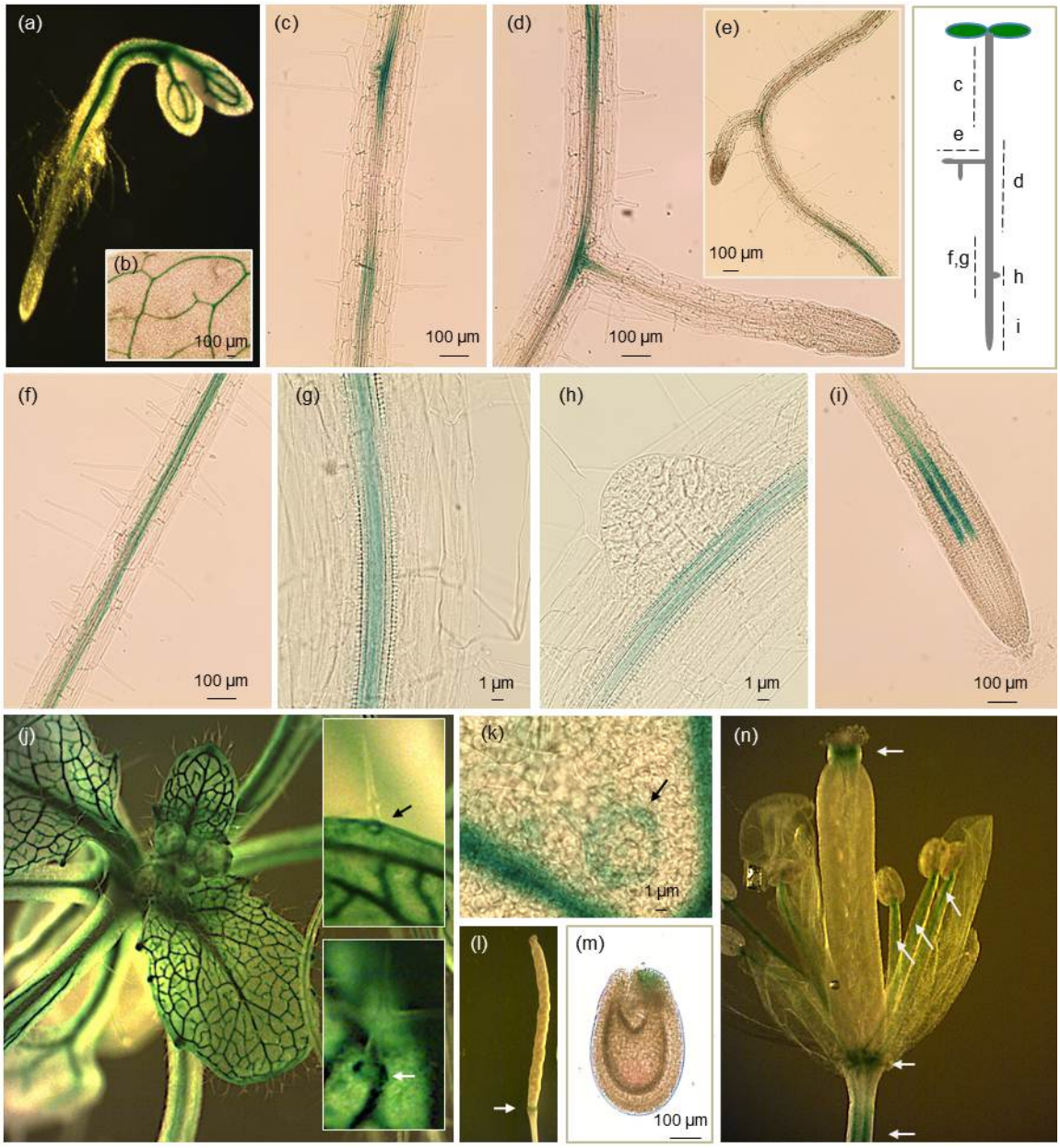

Figure 2. *PLC3$_{pro}$:GUS-YFP* expression analyses in Arabidopis seedlings and mature tissues.
GUS activity was present in the vasculature of 2-d old- (a) and 10-d old seedlings including, shoot and root (b-i). GUS staining was also observed in vascular tissue of mature plants (j), trichome base (indicated by arrows) (j, k), hydathodes (j), silique (l), developing seed chalaza (m) and different parts of the flower (n), including style, filament, receptacle and pedicel (indicated by arrows).

Analysis of PPI-, PA- and IP_6 levels in Arabidopsis seedlings

To determine whether loss-of-*PLC3* caused changes in the level of PLC substrates (i.e. PIP and PIP_2) or products (i.e IP_6 or other IPPs), various isotope labelling studies were performed. Since PLC-generated DAG can be rapidly converted into PA(Munnik *et al.*, 1998; Ruelland *et al.*, 2002; Arisz *et al.*, 2009, 2013), we also measured PA levels. Lipids were analyzed by labelling five-day-old seedlings O/N with $^{32}P_i$. As shown in Figures 3a and 3b, wt and *plc3* seedlings were found to contain similar amounts of PIP_2, PIP and PA. For the IPP analyses, ^{3}H-Inositol labelling of seedlings and HPLC analyses were performed, but also here, no significant changes in the level of IP_6 or lower IPPs were found. On closer inspection of the extremely low levels of the pyrophosphate-IPPs (PP-IPPs), i.e IP_7 and IP_8, we did observe some differences, however. Both *plc3* mutants were found to contain ~30% less IP_8 than wt (Fig. 3d). While the latter analyses were performed on seedlings of 18-days old (11d + 7d of labelling), we also tested younger seedlings with shorter labelling times (4d old + 4d labelling). Again no differences in IPPs were found but in this case, *plc3* mutants were found to contain ~30-40% less IP_7 (see Supplemental Fig. S4).

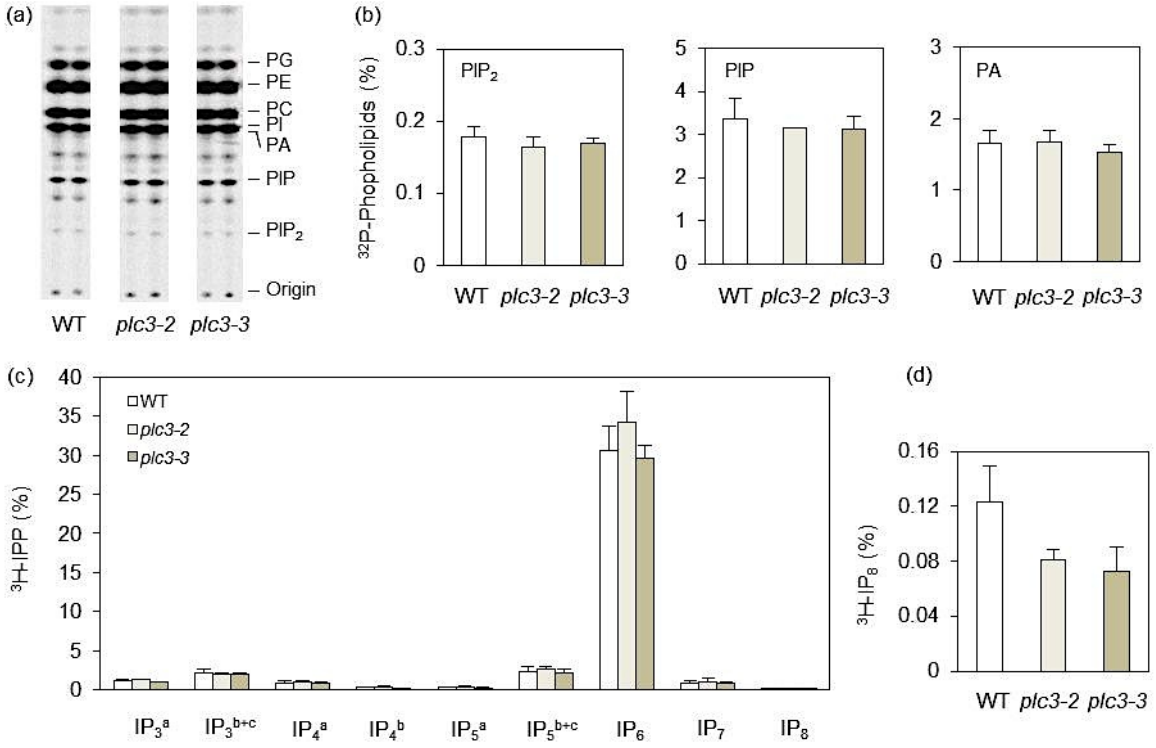

Figure 3. PPI-, PA- and IPP levels in wild type- and *plc3*-mutant seedlings.
For lipid analyses, five-days old seedlings were labelled with $^{32}PO_4^{3-}$ overnight and the next day their lipids were extracted and separated by TLC. (a) Autoradiograph of a typical experiment. Each lane represents the extract of 3 seedlings. (b) Quantification of ^{32}P-labeled PIP_2-, PIP- and PA levels in wild-type and *plc3* mutants. Values are calculated as the percentage of total ^{32}P-labeled phospholipids and represented as means ± SD (n=3). This experiment was repeated twice with similar results (c) Inositol polyphosphates (IPP) levels in wild type and *plc3*-mutant seedlings. (d) IP_8 in wild type and *plc3*-mutant seedlings. Eleven-day old seedlings were labelled with ^{3}H-*myo*-inositol for 7 days, after which the IPPs were extracted and resolved by HPLC-SAX chromatography. Fractions were collected every minute, and the radioactivity was determined by liquid scintillation counting. The quantities are expressed as percentage of total. Data shown are the means ± SD (n=10) of one representative experiment. Similar results were obtained in an independent experiment.

Loss of *PLC3* affects seed germination

We noticed another subtle phenotype: *plc3* mutants always germinated slower on agar plates. Normally, we imbibed seeds on ½MS plates in the dark at 4 °C for 48 h, after which they are transferred to the light. After 24 h in the light, *plc3-2* and *plc3-3* mutants had germinated 54% and 60% less than wt, respectively, and after 28 h this was 17% and 34% (Fig. 4a). These results also primed us to check the *pPLC3::GUS* expression during seed germination. As shown in Fig. 4b, GUS activity was found during testa rupture and radical emergence in the embryo cotyledons and shoot apical meristem, confirming a role for *PLC3* in seed germination.

To investigate whether this was due to changes in sugar quantity or composition, soluble carbohydrates in *plc3* mutants and wt seeds were measured. As shown in Fig. 4C, small changes in trehalose and stachyose were observed, but these differences were not found to be significant ($P<0.05$). Data from three different seed batches was analysed.

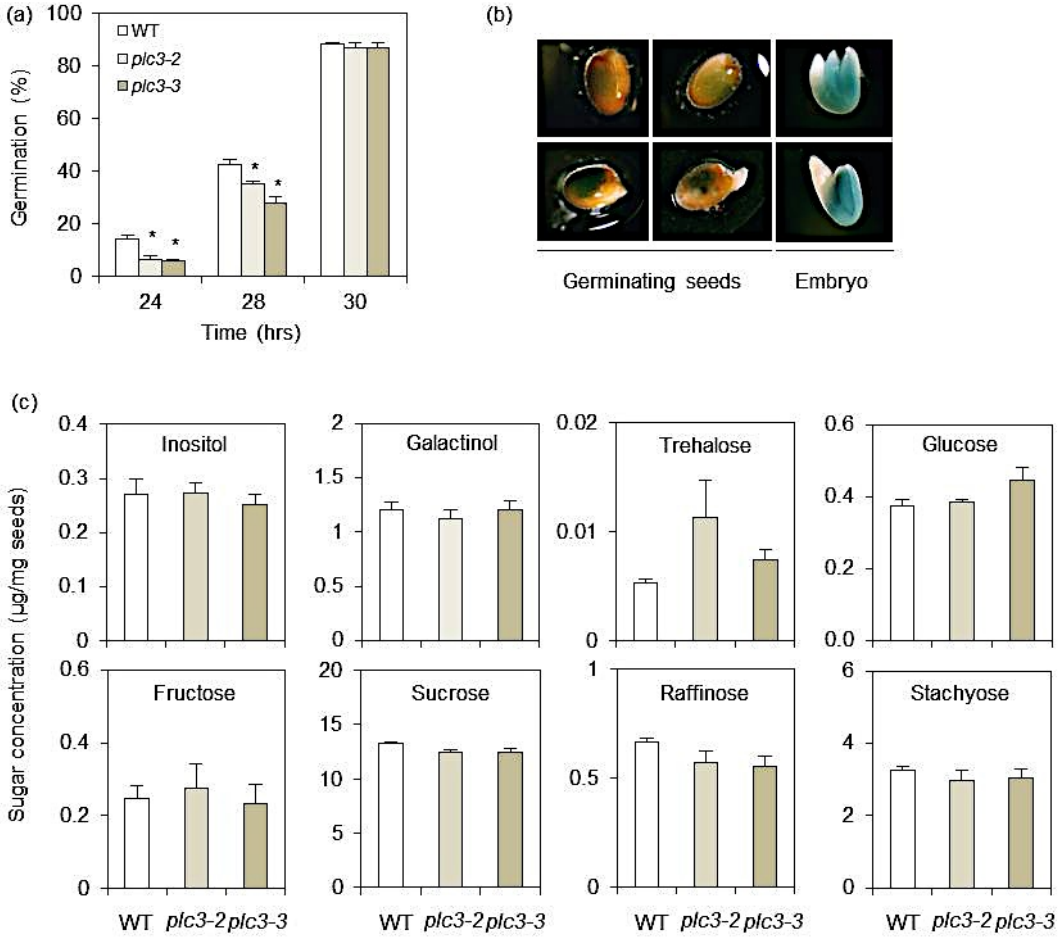

Figure 4. *PLC3* is expressed in germinating seeds and *plc3* mutants exhibit a delayed germination rate and soluble carbohydrates content in seeds of wild-type and *plc3* mutants

(a) Seed-germination rate was determined by radical emergence and scored in wild-type and *plc3* mutants. Seeds were stratified on ½MS with 0.5% sucrose plates at 4°C for 2 days and allowed to germinate at 22°C. Data shown are the means ± SD for one representative experiment (n=55 seeds for each genotype). Asterisks (*) mark that *plc3* values are significantly different from wild-type based on Student's *t-test* ($P< 0.05$). (b) GUS activity was determined in embryo cotyledons during seed germination from testa rupture until radical emergence (20-28hrs after transfer from 4°C to 22°C). These experiment were repeated twice with similar outcome. (c) Soluble carbohydrates were extracted from dry seeds and analyzed by Dionex HPLC. Sugar quantities were corrected by means of an internal standard and transformed to µg of sugar per mg of dry material. Values are the means of triplicates ± SE of three independent seed batches.

Decreased sensitivity to ABA in *plc3* mutants

Since germination could involve ABA sensitivity, this was analysed in more detail. Wild type and *plc3* mutants were germinated on ½MS plates containing different concentrations of ABA (0, 1 and 2 µM). In the absence of ABA, *plc3* mutants germinated slower than wt as described above (Fig. 4a). However, in the presence of ABA, *plc3* mutants were found to germinate faster than wt (Fig. 5a). For example, after 40 h at 1 µM ABA, 12.5% of *plc3-2* and 10.5% of *plc3-3* seeds had germinated whereas only 2.5% of the wt seeds. In time, these differences remained or even increased (Fig. 5a, left panel). At higher ABA concentrations (2 µM), seed germination was inhibited more strongly, but again, both *plc3* mutants had higher germination rates than wt (Fig. 5a, right panel). These results indicated that *plc3* mutants are less sensitive to ABA during germination.

Since ABA is also involved in guard-cell closure (Munemasa *et al.*, 2015), and since antisense-PLC expression in *Nicotiana tabacum* had been shown to reduce the stomatal-closure response upon ABA treatment (Hunt *et al*., 2003), we decided to investigate this further for PLC3. As shown in Fig. 5b, GUS activity of the *pPLC3::GUS* line indicated that *PLC3* was indeed active in guard cells. To investigate its putative involvement in ABA-induced stomatal closure, epidermal peels of wt and *plc3* mutants were treated with different concentrations of ABA (i.e. 0, 0.1, 1 and 10 µM). In the absence of ABA, no significant differences in the stomatal aperture between wild type and *plc3* mutants were found (Fig. 5c). However, with increasing concentrations of ABA, both *plc3-2* and *plc3-3* showed reduced closure responses compared to wt. In summary, these results indicate that loss-of-*PLC3* leads to decreased sensitivity to ABA, in both germinating seeds and guard cells.

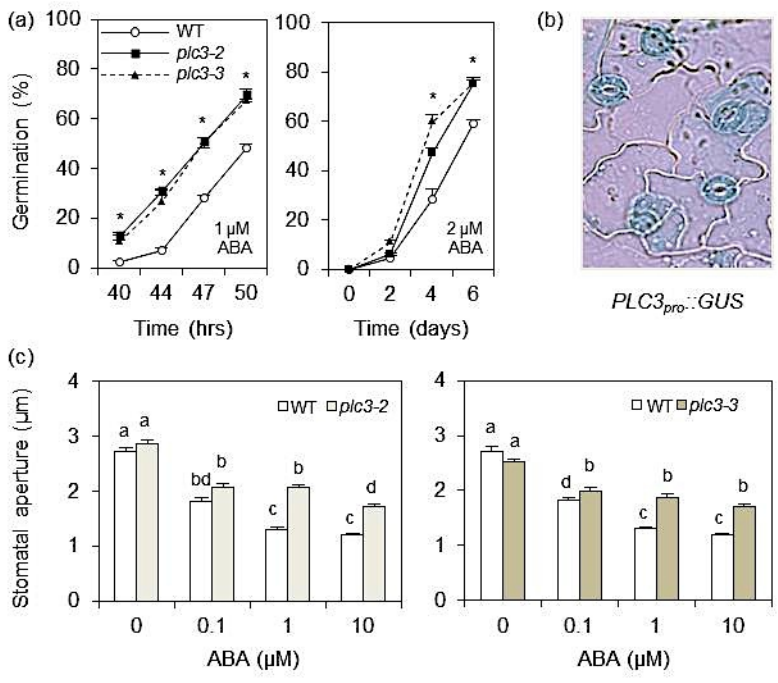

Figure 5. Decreased ABA sensitivity of *plc3* mutants in seed germination and stomatal movement.
(a) Seeds germination rate of wild-type and *plc3* mutants in the presence of 1 or 2 µM ABA. Seeds were germinated on ½MS with 0.5% sucrose plates with different concentration of ABA at 22 °C after 2 days of stratification at 4 °C. Germination is defined by radical emergence and was scored at the indicated times. Data shown are the means ± SD from one representative experiment of at least 3 experiments (n=55 seeds for each genotype). Asterisks (*) mark that *plc3* value are significantly different from wild-type based on Student's *t-test* (P< 0.05). This experiment was repeated 3 times with similar results. (b) $PLC3_{pro}$*:GUS-YFP* expression in guard cells, using epidermal leaf peels of 3 weeks-old Arabidopsis plants . (c) Effect of ABA on stomatal aperture in wild-type and *plc3-2* (left) or *plc3-3* (right). Epidermal strips were incubated in opening buffer with light for 3 h until stomata were fully open. Strips were then treated with different concentration of ABA for 90 mins, after which stomata were digitized and the aperture width measured. Data was analyzed by 2-way ANOVA. Statistically significant differences between genotypes are indicated by letters (P<0.05, Dunn's method). Values are means ± SE of at least three independent experiments (n ≥ 100).

ABA triggers PIP_2 formation in germinating seeds, seedlings and guard cells

Since loss-of-*PLC3* increased the ABA insensitivity during seed germination and stomatal closure, we decided to analyse the phospholipid levels in more detail in these tissues and to analyse the effect of ABA. First the effect in germinating seeds was analysed (Fig. 6). In the absence of ABA, no major differences in the structural phospholipids (not shown) or PIP and PA (Fig. 6a, b) were found between wild type and *plc3* mutants. However, PIP_2 levels in *plc3* mutants were significantly higher than in wild type seeds (i.e. 23% and 22% for *plc3-2* and *plc3-3*, respectively). Upon ABA treatment, no major changes in PIP or PA were found (Fig. 6a, b). However, while a significant increase in PIP_2 (27%) was found in wild-type seedlings upon ABA treatment, both *plc3* mutants lacked this response (Fig. 6b).

Figure 6. PPI- and PA levels in germinating seeds and effect of ABA in wild type and *plc3* mutants.

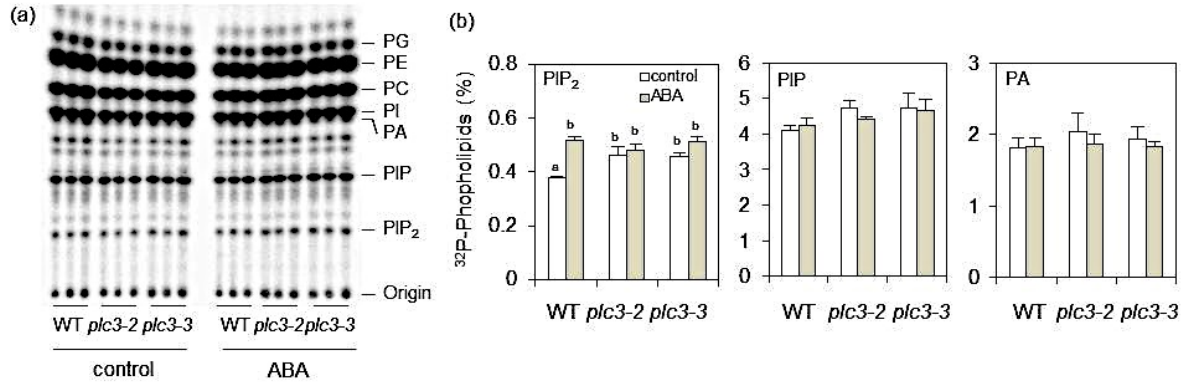

Seeds of wild-type and *plc3* mutants were pre-germinated on ½ MS with 0.5% sucrose plates until testa ruptured, then labelled with $^{32}PO_4^{3-}$ for 24 h, after which they were treated for 2 h with buffer ± 100 µM ABA. (a) Autoradiograph of a typical experiment is shown, each lane representing the extract of ± 200 seeds. (b) Quantification of the ^{32}P-levels of PIP_2, PIP and PA. Three independent experiments were performed; data shown are means ± SD (n=3) from one representative experiment. Data was analyzed by 2-way ANOVA. Statistical significant differences between genotypes are indicated by letters ($P<0.05$, Dunn's method).

Next, we analysed the response in guard cells (Fig. 7). For this we used epidermal-leaf peels that are enriched in guard cells (Munnik & Laxalt, 2013) from wt and mutant leaves, and labelled these with $^{32}P_i$ for 3 hrs. Longer labelling times were found to have a negative effect on the viability of the guard cells (not shown). Similar to what we found for germinating seeds, *plc3* mutants contained slightly higher PIP_2 levels (Fig. 7), while PIP and PA and the major structural phospholipids levels remained unchanged (Fig. 7; not shown). With ABA (15 min treatment), again a significant increase of PIP_2 was observed for wild type, but not in the *plc3* mutants (Fig. 7). A small decrease in PIP and increase in PA was found, but these changes were not statistically significant ($P<0.05$). No changes in the structural phospholipids were found. We also tested the effect of ABA after 2, 5, 30 and 60 min, but no clear differences were found before or after treatment in both wild type and *plc3* mutants.

Similarly, the effect of ABA on seedlings was analysed. Time-course analyses in wt seedlings revealed an increase in PIP_2, which was found to be significant after ~30-60 min of treatment (Supplemental Fig. S6). PIP, PA and structural-phospholipids levels remained the same during that period (Supplemental Fig. S6 b-d). Testing *plc3* mutants after 1 h of ABA treatment showed in this case

an accumulation of PIP_2, which was not significantly different from wild type (Supplemental Fig. S6f). PIP, PA and structural-phospholipid levels remained similar.

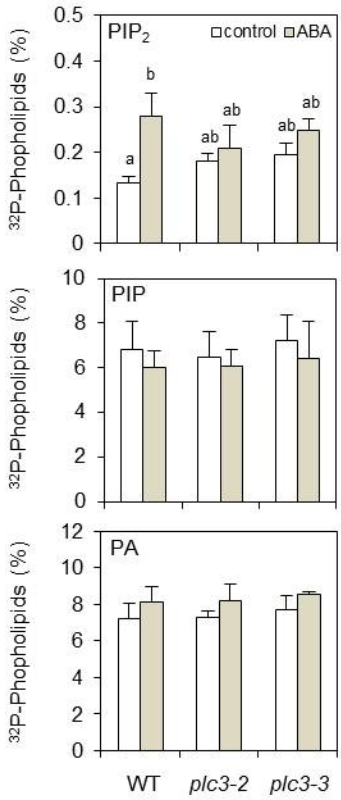

Figure 7. PPI and PA levels in leaf peels and effect of ABA in wild-type and *plc3* mutants.

Three-week-old rosette leaf peels from wild-type and *plc3* mutants were $^{32}P_i$-labeled for 3h and then treated in buffer ± 100 µM ABA for 15 min. Lipids were then extracted and separated by TLC. Radioactivity levels in PIP_2, PIP and PA were determined as percentage of total phospholipids. Three independent experiments were performed. Data shown are the means ± SD (n=3) from one representative experiment. Data was analyzed by 2-way ANOVA. Statistical significant differences between genotypes are indicated by letters ($P<0.05$, Dunn's method).

Over expression of *PLC3* enhances drought tolerance

Overexpression of *PLC* has been shown to promote drought tolerance in maize, canola and tobacco (Wang *et al.*, 2008; Georges *et al.*, 2009; Tripathy *et al.*, 2011). It is unknown whether specific PLCs were chosen for this or whether any PLC can achieve this. For Arabidopsis, this is unknown either. Hence, we generated transgenic plants overexpressing *PLC3* under the control of the *UBQ10* promoter. Transgenic plants were selected from T0 to T3 and independent homozygous lines were obtained.

Two homozygous lines, *PLC3-OE9* and PLC3-*OE16*, were selected for further studies, overexpressing *PLC3* 48-fold and 20-fold, respectively (Fig. 8a). No obvious phenotypes were observed comparing wild type and the *PLC-OE* lines on either agar plates or soil. In soil, four weeks old plants from PLC3-OE lines were found to be more drought tolerant than wt (Fig. 8b) and to show significantly higher survival rates (Fig. 8b, c).

During drought stress, the shoot FW of wild type decreased by ~21%, which was less in the *PLC3-OE9* and *PLC3-OE16* lines (17% and 12%, respectively)(Fig. 8d). Their DW, however, was higher with or without drought (Fig. 8e). *PLC3*-overexpression lines also lost less water when water loss of detached 4-week-old rosettes were compared (Fig. 8f).

ABA synthesis is stimulated by dehydration stress and known to induce stomatal closure to reduce water loss (Sean *et al.*, 2010). In the absence of ABA, stomatal aperture of *PLC3-OE*s was found to be strongly reduced by ~30%. Upon ABA treatment (0.1 µM), stomata closed rapidly for all

genotypes, but the aperture of the *PLC3-OE*s was still significantly smaller than wild type. Above 1 µM, this difference was not observed (Fig. 8g).

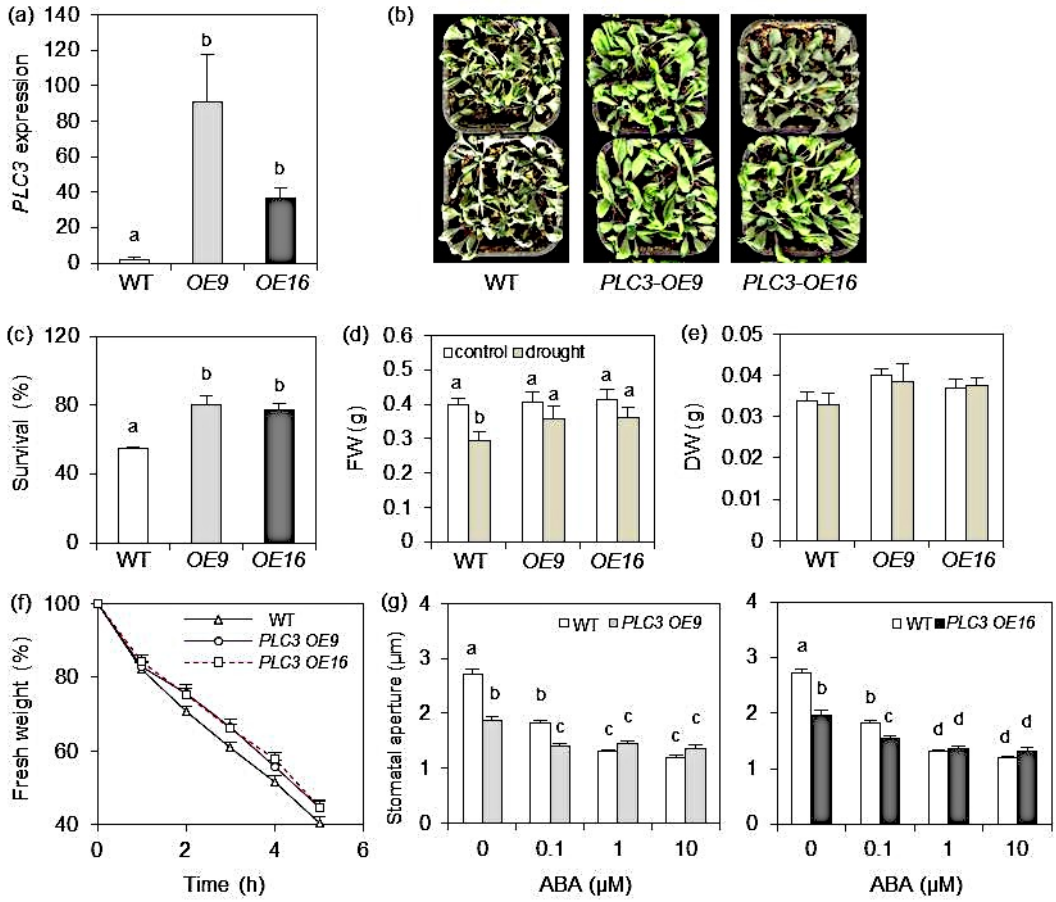

Figure 8. Overexpression of *PLC3* enhances drought tolerance.
(a) *PLC3* expression levels in wild-type and two homozygous PLC3 overexpression lines, *PLC3-OE9* and *PLC3-OE16* as measured by Q-PCR and based on the expression of the *SAND* reference gene. Values are means ± SD (n = 3) for one experiment. (b) Phenotype of wild type- and *PLC3-OE* plants. Four-week old soil-grown plants were exposed to drought stress by water withholding for 2 weeks. (c) Survival rates were determined by counting the visible, green plants after re-watering. (d, e) Fresh- and dry weights were determined from shoots under control and drought (1 week water withholding) conditions. (f) Water loss of detached rosette. Water loss was measured at indicated time points and expressed as a percentage of the initial fresh weight. Values are means ± SD for one representative experiment (n=36). (g) ABA-induced stomatal closure in wild-type, *PLC3 OE9* (left), *PLC3 OE16* (right) plants. Epidermal peels from 3-weeks old plants incubated in opening buffer with light for 3 h until stomata were fully open. Peels were then treated with different concentration of ABA for 90 mins, after which stomata were digitized and the aperture width measured. Values are means ± SE of at least three independents (n >100). Data was analyzed by 2-way ANOVA. Statistical significant differences between genotypes are indicated by letters ($P<0.05$, Dunn's method).

Higher accumulation of PIP_2 in *PLC3* overexpressing plants under osmotic stress

To determine whether overexpression of *PLC3* caused any changes in PPI- and/or PA levels, ^{32}P-labelling experiments were performed on seedlings, and the effect of 600 mM sorbitol was tested to mimic water stress. As shown in Fig. 9, no major differences between wild type and *PLC3-OE* lines were found under
control conditions. However, upon sorbitol treatment, a much stronger PIP_2 response was observed in the OE lines. In wt, PIP_2 levels increased by about 300%, while in the OE lines a ~600% increase was witnessed. The PA response appeared slightly higher (200% vs 300%) but this was not statistically significant. The osmotic stress-induced decrease in PIP was similar to wild type (Fig. 9b). These results suggest that *PLC3-OE* lines are capable of enhancing the PIP_2 response under osmotic stress.

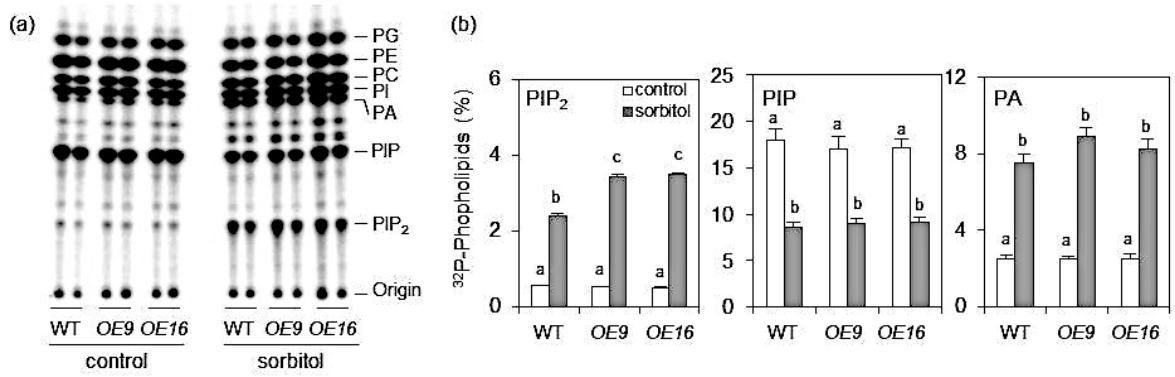

Figure 9. Osmotic stress triggers PIP_2 and PA responses in wild type- and *PLC3-OE* seedlings.
Six-day-old seedlings were ^{32}P-labeled for 3h and then treated with buffer ± 600 mM sorbitol for another 30 min. Extracted lipids were analyzed by TLC and quantified through phosphoimaging. (a) Typical TLC profile with each lane representing the extract of 3 seedlings. (b) ^{32}P-levels in PIP_2, PIP and PA of wild-type and *PLC3-OE lines #9* and *#16* with anbd without sorbitol. Three independent experiments were performed. Data shown are the means ± SE (n=3) from three independent experiments. Data was analyzed by 2-way ANOVA. Statistical significant differences between genotypes are indicated by letters ($P<0.05$).

DISCUSSION

In this paper, new roles for PLC in plant stress and development are described. Using loss-of-function mutants in Arabidopsis, we found that *AtPLC3* is involved in seed germination, root development, stomatal movement and ABA signaling, whereas overexpression of *PLC3* enhanced the plant's tolerance to drought stress. While these findings underline the importance of PLC signaling in plant stress and development, we still know very little of how this is achieved at the molecular level. Theoretically, there are several possibilities. First of all, PLC can produce DAG and IP_2 or IP_3, (depending on whether PIP or PIP_2 is used as a PLC substrate), and while plants lack the classical targets of the mammalian paradigm (i.e. IP_3 receptor, PKC), it is likely that their phosphorylated products, i.e. PA and higher IPPs (incl. PP-IPPs) fulfill this second-messenger role in plants. Various biological processes have already been linked to these molecules, and several protein targets involved in signal transduction and metabolism have been identified too (see below). In guard cells, IP_6 has been show to release Ca^{2+} (Lemtiri-Chlieh *et al.*, 2000, 2003), so the PLC system in plants could potentially do that.

In non-stressed cells, it is more likely that PLC will hydrolyse PIP than PIP_2. The concentration of the latter in plasma membranes is extremely low in plants (30-100 fold lower than mammalians; Munnik *et al*., 1994; Meijer and Munnik, 2003), while PI4P concentrations appear comparable to those found in mammalian cells (Munnik, 2014). Moreover, in order to make IP_6 out of IP_2 or IP_3 involves the same two inositolpolyphosphate kinases (IPKs). IPK2 is an inositol multiphosphate kinase that can phosphorylate the 3-, 5-, and 6- position of the inositol ring to produce IP_5. IPK1 specifically phosphorylates IP_5 at the 2-position to produce IP_6. VIH2 is a recently discovered IPK that is responsible for the production of the pyrophosphorylated IPPs, i.e. IP_8. Like in animal- and yeast cells, these compounds are emerging as important signaling molecules in plants (York, 2006; Michell, 2008; Burton *et al.*, 2009; Shears, 2009; Desai *et al.*, 2014; Laha *et al.*, 2015).

Another function of PLC could be to attenuate PIP_2 signalling. While the concentration of this lipid is extremely low under control conditions, PIP_2 is readily produced in response to certain hormones or stress signals, where it is suggested to fulfill a second messenger itself, regulating various aspects of plant growth, development, and stress signaling (Gillaspy, 2013; Rodriguez-Villalon *et al*., 2015; Heilmann, 2016; Zarza *et al*., unpublished). Potential targets include proteins involved in ion transport (e.g. K^+ channels), membrane trafficking (endo/exocytosis, e.g. clathrin and Exo70) and cytoskeletal organization (e.g. small G-protein, Rop) (Gillaspy, 2013; Munnik, 2014; Heilmann, 2016). *In vitro,* plant PLCs hydrolyze PI4P and $PI(4,5)P_2$ equally well (Munnik, 2014), and since PI4P is emerging as a lipid second messenger too (Vermeer *et al*., 2009; Munnik and Nielsen, 2011; Heilmann, 2016), under certain conditions and in particular cells, PLC could also function as attenuator of PI4P signalling. As far as we know, PLCs are unable to use D3-phosphorylated inositol lipids as a substrate [i.e. PI3P and $PI(3,5)P_2$] or PI5P (Munnik, 2014). Whether the newly linked-PLC3 functions observed

here, reflect PLC's role as second messenger producer or -attenuator (or both), needs to be established. Below, a broader perspective of our results is given and some potential molecular mechanisms discussed.

Role for *PLC3* in seed germination

Promoter-GUS expression in germinating seeds (Fig. 4b), together with the delayed germination phenotype of both *plc3* mutants (Fig. 4a), indicates a role for PLC3 in seed germination. Since ABA is known to play an important role in this (Nambara *et al*., 2010; Nakashima & Yamaguchi-Shinozaki, 2013), we investigated whether the delayed germination of the *plc3* seeds was caused by hypersensitivity to ABA. Surprisingly, *plc3* mutants were found to be less sensitive to ABA (Fig. 5a). Such results are in agreement with Sanchez & Chua (2001), who found that the ABA sensitivity of seed germination and downstream-gene expression was lost when *PLC1* was silenced in Arabidopsis. Guard cells of *plc3* mutants were also found to be less sensitive to ABA, which could point to a more general role for PLC3 in ABA signaling (see below; Fig. 5). At least, the above results indicate that the basal, delayed germination rate in *plc3* mutants is unlikely to be caused by ABA hypersensitivity.

Gibberellin (GA) is another important hormone involved in seed germination (Yamaguchi and Kamiya, 2001). In contrast to ABA, GA promotes seed germination, and there is data to suggest that this could involve PLC signaling too, i.e. induced *PLC* expression, changes in PPIs, and increased IP_3 levels (Murthy *et al*., 1989; Chen *et al*., 1997; Kashem *et al*., 2000; Villasuso *et al*., 2003; Fleet *et al*., 2009; Luo *et al*., 2012). We tested whether *plc3* mutants were affected in GA responsiveness by comparing their germination to wt, with and without 1 mM GA (Supplemental Fig. S7). Although the initial germination rate of *plc3-2* and *plc3-3* mutants with GA was still slower than wild type (Supplemental Fig. S7a and b), after 24h, the fold-increase in *plc3* mutants was around 20% more than in wild type. This was found in three independent experiments, despite the fact that the difference was not statistically significant (Supplemental Fig. S7c). These results point to a possible role for *PLC3* in GA signaling, even though the hypersensitivity of the *plc3* mutants to GA does not explain their slower germination phenotype. One hypothesis could be that PLC has a positive effect on GA levels and therefor lower GA levels in the mutant, which could delay germination. By adding external GA, some of this inhibition might then be released, which would become visible as hypersensitivity.

Results from our phospholipid measurements revealed that germinating *plc3* seeds contained significantly higher levels of PIP_2 (Fig. 6), which would be consistent with a loss of *PLC3* that would normally hydrolyze this lipid to produce IP_3. Unfortunately, the latter is very difficult to measure because seeds contain tiny amounts of IP_3 and huge amounts of IP_6, and are also extremely difficult to label with ^{3}H-inositol (Stevenson-Paulik *et al.*, 2005). Seeds hardly take-up this label, and this is probably also the reason why young seedlings require relatively long labelling times (i.e. 4-11 days vs hrs with $^{32}P_i$; see Methods). Seeds typically store high amounts of IP_6 during their development, where it is used as supply of phosphate (e.g. for DNA, ATP, membranes and sugars) and inositol (IPPs, PPIs,

precursor of cell wall sugars) (Munnik and Nielsen, 2011; Valluru and Van den Ende, 2011) when the seed germinates and the embryo develops into a seedling while growing in the dark. This so-called 'storage' IP_6 is easily confused with 'signalling' IP_6 (Munnik and Vermeer, 2010), but has totally different functions and is probably even differentially localized within cells or tissues. It is difficult, if not impossible, to distinguish between these two IP_6 sources at the moment (Munnik and Vermeer, 2010; Gillaspy, 2011; Munnik and Nielsen, 2011). During seed germination, IP_6 is rapidly broken down to IP_3 (Luo *et al.*, 2012) and this could be an alternative explanation for what was assumed to be PLC-generated IP_3 (Murthy *et al*., 1989; Chen *et al*., 1997; Kashem *et al*., 2000; Villasuso *et al*., 2003; Fleet *et al*., 2009; Luo *et al*., 2012).

Another set of molecules related to inositol metabolism are Raffinose Family Oligosaccharides (RFOs), which serve as desiccation protectant in seeds, as transport sugar in the phloem and as storage sugar in various tissues (Sengupta *et al.*, 2015). In Arabidopsis seeds, RFOs are required for the rapid germination in the dark (Gangl and Tenhaken, 2016). RFOs are sucrose derivatives to which a galactosyl unit is attached via galactinol (Gol). The latter is produced via UDP-galactose and *myo*-inositol by the enzyme, galactinol synthase (GolS). To make RFOs, free *myo*-inositol is required and this is predominantly formed through cyclization of glycolytic glucose 6-phosphate (G6P) into inositol-3-phosphate (Ins3P) by myo-inositol-3-phosphate synthase (MIPS) and subsequent dephosphorylation by inositol mono- phosphatase (InsPase). Theoretically, however, inositol could also be generated via dephosphorylation of PLC-generated IPPs (Munnik and Vermeer, 2010). We analysed the soluble carbohydrate composition in seeds and in the phloem sap but found no significant differences between wt and *plc3* mutants. Of course, changes could be very local so it is possible these differences remain unobserved.

During seed development, *PLC3* was expressed at the chalaza, the non-micropylar end of the seed, likely the chalaza endosperm and/or seed coat (Fig. 2m). Nutrients from the mother plant are transported via the vascular tissue through the chalaza into the nucellus. The vascular and chalaza expression of PLC3 might be necessary for nutrient transportation. Alternatively, PLC might be involved in the production of IP_6 for the storage of essential minerals. Developing seeds store these minerals in three locations, i.e. in the protein storage vacuoles of the embryo, and transiently in the endoplasmic reticulum (ER) and vacuolar compartments of the chalaza endosperm. X-ray analysis and enzyme treatments have suggested that these minerals are stored as IP_6-salts with distinct cation (Mg, Mn, Zn, K, and Ca) composition per compartment (Otegui *et al.*, 2002). As such, loss of *PLC3* may affect embryo development, germination and even plant development.

Role for *PLC3* in lateral root formation and auxin signaling

Loss-of-function *PLC3* mutants displayed shorter primary roots and fewer lateral roots (Fig. 1). The latter was due to less initiation sites, not development (data not shown). Promoter-GUS analyses indicated a very typical, segmented, *PLC3*-expression pattern at the lateral root-emerging site, whereby

lateral roots always emerged from a segment, but not every segment resulted in a lateral root. Normally, we grow our plates vertically in an angle of 70°. By tilting the agar plate more horizontally (45°), roots start to wiggle more and tend to grow a lateral root at every bend. Using the latter setup for GUS analyses, revealed that lateral roots only emerged from these segments, but that the number of segments was drastically reduced, which was almost 1:1 with the lateral roots whereas with the 70° setup, typically two or three segments were found near the lateral root. These results may indicate that *PLC3* expression is required just before the lateral root is initiated, and that the primary root at the 70° setup is less determined as to where and when it will produce the lateral root compared to the 45° setup where this decision is forced at the bending sites (Ditengou *et al.*, 2008). That the phenotype is quite mild may indicate that redundant PLCs are involved. Using the eFP browser data, we found that in addition to *PLC3*, expression of *PLC2*, *PLC5* and *PLC7* is also present in the phloem and/or companion cells.

Interestingly, the initiation of tertiary roots revealed a very similar GUS-expression pattern, showing segments in the lateral roots from which tertiary roots emerged. Root growth and -branching are main events of root development. Root growth requires cell proliferation and division in the meristematic zone, and cell expansion in the elongation zone. Lateral root formation involves three major steps, which are initiation, primordial organogenesis, and emergence (Benková and Bielach, 2010). Auxin has been shown to be required in both primary root growth and lateral root formation (Péret, De Rybel, *et al.*, 2009; Péret, Larrieu, *et al.*, 2009; Benková and Bielach, 2010). The signaling pathway of auxin perception is well characterized. Auxin promotes the degradation of the transcriptional repressor Aux/IAA, resulting in massive auxin responsive-gene expression. The auxin receptor, TIR1 is a F-box protein and complex with SCF (ubiquitin protein ligase), which promotes ubiquitin-dependent proteolysis of Aux/IAAs (Kepinski and Leyser, 2005). Interestingly, IP_6 has recently been found in the crystal structure of TIR1 where it is thought to be required for auxin binding and TIR1 function (Tan *et al.*, 2007). Where the IP_6 is coming from is unknown, but potentially this could be formed though PLC3-generated IP_2- or IP_3 formation at the above mentioned 'segments' and subsequent phosphorylation into IP_6. Less PLC-generated IP_6 in *plc3* mutants would then lead to less auxin responsiveness during root development (Fig.10A). Redundant *PLCs* are likely to take over most of *PLC3's* function(s) though.

In contrast to the germinating seeds, no differences in PPI- or PA levels were found in $^{32}P_i$-prelabeled seedlings (Fig. 3b). However, since *PLC3* is expressed in a limited number of cells (especially in the phloem companion cells), analyses of whole seedlings might dilute any difference. We also did not find differences in IP_6 either. Tiny differences in the pyro-IPP levels were found, however, with lower levels of IP_7 and IP_8 in the *plc3* mutants depending on their age (Fig. 3c; supplemental Fig. 4). Both IP_7 and IP_8 are implicated as novel signalling molecules (Laha *et al.*, 2015, 2016) for which there is already lots of evidence in yeast and animals (York, 2006; Michell, 2008; Burton *et al.*, 2009; Shears, 2009). That PLC3 could be involved in generating such signaling molecules is exciting, but requires further analysis. Similarly, on the role of IP_6. In guard cells, IP_6 may be

responsible for the release of intracellular Ca^{2+} and since the latter is also important for auxin signaling (Zhang *et al.*, 2011), this line of research is worth perusing too. The main bottleneck, still, after the first discoveries over 25 years ago (Blatt *et al.*, 1990; Gilroy *et al.*, 1990; Allen and Sanders, 1994), is the identification of a genuine IP_6- (or other IPP-) gated channel (Lemtiri-Chlieh *et al.*, 2000, 2003).

As discussed above, PLC3 could also be involved in inositol-based RFO metabolism. Since RFOs are important for carbohydrate transport- and storage, potentially they could be involved in loading sucrose to sink organs, e.g in lateral root (Van den Ende, 2013; Sengupta *et al.*, 2015; Gangl and Tenhaken, 2016). Analysing the sugar composition of the phloem sap revealed increased amounts of sucrose in the *plc3* mutants and slightly decreased levels of *myo*-inositol levels, although the latter differences were not significant (Supplemental Fig. 3b). If sucrose is not properly transported to, or into, the lateral root via a PLC depended-RFO pathway, then sucrose levels could indeed be higher in the phloem sap and theoretically could affect root growth and lateral root formation.

Role for *PLC3* in stomatal closure and ABA signaling

PLC has been linked to ABA signaling in several reports (Hirayama *et al.*, 1995; Sanchez and Chua, 2001; Hunt *et al.*, 2003; Sui *et al.*, 2008). In Arabidopsis, a number of *PLC* genes are induced upon ABA treatment (Hunt *et al.*, 2004; Lin *et al.*, 2004; Tasma *et al.*, 2008). We tested our *plc3* mutants for their response to exogenous ABA with respect to inhibition of seed germination and ABA-mediated stomatal closure along with wild type. Results showed that down-regulation of *PLC3* decreased the ABA sensitivity for both responses (Fig. 5). Similar results have been found for germinating seeds of *PLC1*-silenced Arabidopsis plants (Sanchez and Chua, 2001), and in guard cells of *PLC*-silenced tobacco plants(Hunt *et al.*, 2003; Mills *et al.*, 2004).

We also tested the effect of ABA on the turnover of phospholipids in germinating seeds and guard cell-enriched leaf peels and found an increase of PIP_2 in both tissues after ABA stimulation, which was strongly reduced or even lost in the *plc3* mutants (Figs. 6 and 7). We speculate that PLC3 is activated by ABA, thereby increasing the hydrolysis of PIP_2 and the subsequent replenishment of the pool by PIPK. Increased turnover of PIP_2 is ideally reflected by this type of ^{32}P-labeling experiment (Munnik *et al*., 1994; Munnik and Zarza, 2013).

In Figure 10B, a model is presented of how PLC3 and PIP_2 could be involved in regulating stomatal movement. The latter is controlled by changes in turgor of the surrounding guard cells. During stomatal opening and -closing, ion channels and cytosolic Ca^{2+} oscillations play key roles in this process, and these transporters need to be tightly regulated. Over the years, many genes and proteins have been implicated (Ward *et al*., 2009; Roelfsema *et al*., 2012; Munemasa *et al*., 2015; Assmann and Jegla, 2016). Here, we would like to draw the attention of how PPIs and IPPs could regulate stomatal movement. During light induced-stomatal opening, the H^+-ATPase pump is activated, which causes hyperpolarization of the plasma membrane and the opening of the voltage-gated K^+ - influx channel, KAT1. The subsequent influx of K^+ lowers the water potential and drives the net influx of water into

the guard cell (Dietrich *et al.*, 2001; Schroeder *et al.*, 2001; Ward *et al.*, 2009; Roelfsema *et al.*, 2012). Meanwhile, ABA-INSENSITIVE 1 (ABI1), a type 2C protein phosphatase (PP2C), inhibits SNF1-Related kinase (SnRK2, i.e. OST1) activity, which in its active form activates the slow anion channel 1 (SLAC1). PIP5K4 is essential for stomatal opening (Lee *et al.*, 2007). This lipid kinase generates PIP_2, which has been shown to inhibit SLAC1 (Lee *et al.*, 2007) and the K^+-efflux channel (Ma *et al.*, 2009) co-facilitating the low water potential, the subsequent influx of water, and the opening of stomata.

Upon ABA, the PYR/PYL-receptor dimer dissociates and forms PYR - or PYL-ABA complexes(Ma *et al.*, 2009; Park *et al.*, 2014) that bind PP2C (Melcher *et al.*, 2009; Miyazono *et al.*, 2009; Nishimura, 2009; Santiago *et al.*, 2009; Yin *et al.*, 2009), which can then no longer inhibit the protein kinase activity of SnRK2/OST1 (Hirayama and Umezawa, 2010). As a consequence, OST1 can now auto-phosphorylate itself (Soon *et al.*, 2012) and activate SLAC1 (Kulik *et al.*, 2011), which results in a decrease of intracellular Cl^-. Activated PLC, hydrolyses PIP_2, thereby releasing the inhibition of SLAC1 and the K^+-efflux channel, but also generates increased amounts of IP_3 and IP_6 through IPK1 and IPK2. The IP_6 can release Ca^{2+} from internal stores (Lemtiri-Chlieh *et al.*, 2000, 2003; Munnik, 2014), which inhibits the K^+ - influx channel (Lemtiri-Chlieh *et al.*, 2000) and co-activates SLAC1 (Siegel *et al.*, 2009). Together these activities cause the net efflux of K^+ and Cl^-, which decreases the water potential and causes water to leave the guard cells and stomata to close. PLC3 seems to be one of the PLC genes involved in this process. Although *plc3* mutants still respond to ABA by closing their stomata, the response is significantly reduced. How the PLCs involved are activated still remains elusive. Ca^{2+} is a potential factor since it stimulates PLC activity *in vitro* (Munnik *et al.*, 1998), but this would first require an influx of Ca^{2+} into cytosol via another pathway. As such, PLC and PIP_2 would act as facilitators in these biophysical events. The redundancy of 9 PLCs and 11 PIPKs may prevent more clear phenotypes.

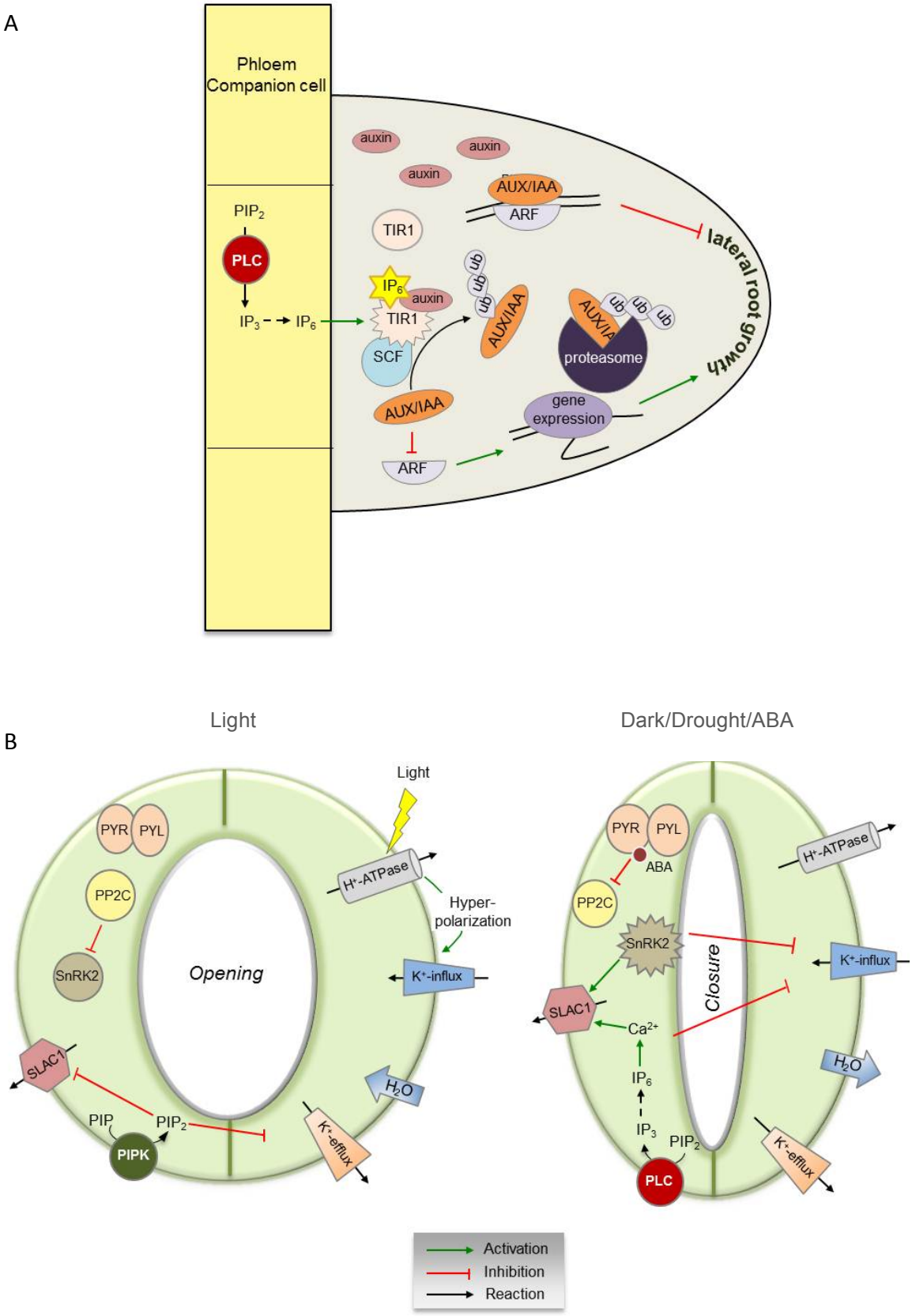

Figure 10. Models for the role of PLC in (A) lateral root formation, and (B) regulating stomatal aperture.
Abbreviations: KAT1: voltage-gated K^+influx channel; ABI1: ABA-INSENSITIVE 1; PP2C: type 2C protein phosphatase; SnRK2: SNF1-Related kinase; SLAC1: slow anion channel 1

Overexpression of *PLC3* enhances drought tolerance

Plants cope with drought stress via many different strategies (Zhu, 2002, 2016; Osakabe *et al.*, 2013; Mickelbart *et al.*, 2015) and recently various lipid signalling pathways have been reported to be involved in (Munnik and Meijer, 2001; Zhu, 2002; Meijer and Munnik, 2003; Munnik and Vermeer, 2010; Hou *et al.*, 2016). Moreover, overexpression of a *PLC* in maize, tobacco and canola have been shown to improve drought tolerance (Wang *et al.*, 2008; Georges *et al.*, 2009; Tripathy *et al.*, 2011). To investigate whether overexpression of Arabidopsis *PLC3* could advance drought tolerance, homozygous *pUBQ10::PLC3* overexpression lines were generated. Under control conditions, these plants appeared similar to wild type, but upon drought stress the *PLC3-OE* lines clearly performed better (Fig. 8b, 8c). They lose less water than wild type, which is likely due to increased number of closed stomata, as there was no difference in stomata number. The molecular mechanism behind this may well reflect what we discussed above and what is summarized in Figure 10.

In an attempt to mimic this in seedlings by using sorbitol, we found that PIP_2 and PA accumulated dramatically upon this water stress, and that the accumulation was much stronger in the *PLC3-OE* lines (Fig. 9). This may again reflect the increased turnover of PIP_2 and phosphorylation of DAG, which is readily picked-up by these ^{32}P-labelling experiments. We also measured IPP levels with ^{3}H-inositol labeling, but found no differences there between wt and *PLC3-OE* lines.

Besides guard-cell regulation, PA and PIP_2 may accumulate in various other cells and tissues, since the UBQ10 promoter is constitutively expressed, which is totally different from the endogenous PLC3 expression in the vasculature. Both lipids have been implicated as second messengers, playing roles in reorganization of the cytoskeleton, endo- and exocytosis, vesicular trafficking and ion channel regulation (Stevenson *et al.*, 2000; Martin, 2001; van Leeuwen *et al.*, 2007; Heilmann, 2016), which are all important cellular events. Therefore, PIP_2 and PA are very likely to play an important role in the plant's response to control water stress. Further unraveling of the molecular mechanisms involved here requires identification and characterization of some of the main targets of these lipid second messengers, but also for the IPPs, with IP_6 and the PP-IPPs in particular. How PLC is activated remains also an important issue to address.

Apart from osmotic stress, heat stress also triggers a PIP_2 and PA responses (Mishkind *et al.*, 2009; Horvath *et al.*, 2012). Recently *AtPLC3* and *AtPLC9* were claimed to be involved in heat stress. Their T-DNA insertion lines lacked the IP_3 response and exhibited decreased thermotolerance while overexpression lines showed more heat resistance (Zheng *et al.*, 2012; Gao *et al.*, 2014). Problem here is *AtPLC9* is predicted to be “non-active” due to the lack of conserved amino acids in the X-Y domain that are required for the catalytic activity (Hunt *et al.*, 2004). IP_3 was measured with the commercial displacement assay, this may reflect changes in the flux of other IPPs (Munnik, 2014). However, if the inactive AtPLC9 could bind PIP_2, then its competition with active PLCs might regulate PIP_2’s function as a second messenger.

For many years, PLC/IP_3/Ca^{2+} pathway has been claimed to involved in gravitropism (Perera *et al.*, 1999, 2006; Stevenson *et al.*, 2000; Boss *et al.*, 2010). We tested our *plc3* mutants response to gravitropism by changing the root growth direction (rotate the plate by 90°; Supplemental Fig. S8 a,b). The roots of both wild type and *plc3* mutants bended around 90°due to gravitropism and no obvious difference in bending degree between them (Supplemental Fig. S8c). The reason could be *PLCs* redundancy. However, most evidence for PLC/IP_3/Ca^{2+} enrollment in gravitropism is based on IP_3 measurements using the commercial IP_3- displacement kit, which might reflect the flux of other IPPs as well (Munnik, 2014). This is equally interesting and deserves further investigation.

MATERIALS AND METHODS

Plant material

Arabidopsis thaliana (Columbia-0) T-DNA insertion mutants *plc3-2* (SALK_037453) and *plc3-3* (SALK_054406) were obtained from SALK collection (signal.salk.edu). Homozygous plants were identified by PCR in F2 generation by using gene-specific primers in combination with left border primer LBa (Supplemental Table1).

RNA extraction and RT-PCR

The expression levels of *plc3* mutants were confirmed by RT-PCR. Total RNA was extracted with Trizol reagent (Invitrogen, Carlsbad, CA) as described previously (Pieterse, 1998). RNA (5 μg) was converted to cDNA using oligo-dT18 primers, dNTPs and SuperScript III Reverse Transcriptase (Invitrogen) according to the manufacturer's instructions. *PLC3* and *TUBLINα4* were PCR amplified for 40 and 30 cycles respectively with gene specific primers (Supplemental Table1).

Cloning and plant transformation

To generate the *$PLC3_{pro}$:GUSYFP* fusion, a 2437 bp *PLC3* promoter region was amplified from genomic DNA using *PLC3promHindIIIfw* 5'- CCCAAGCTTCAAGTCGCCGAACGAGACATC-3' and PLC3promNheIrev 5' -CTGCTCTTCTTCTTCTTACTTGTTAG-3' and cloned in *HindIII/XbaI* digested *pJV-GUSYFP*. The *$PLC3_{pro}$:GUSYF* cassette was transferred to pGreen0179 using *NotI*. *MultiSite* Gateway Three-Fragment Vector Construction Kit (www.lifetechnologies.com) was used to generate *$UBQ10_{pro}$:PLC3*, *PLC3* cDNA was cloned into pGreen0125 expression vector. The procedure followed MultiSite Gateway Three-Fragment Vector Construction Kit user guide (https://tools.thermofisher.com/content/sfs/manuals/multisite_gateway_man.pdf). Constructs were transferred into *Agrobacterium tumefaciens* strain GV3101, which was used to transform wild type plant by floral dip (Clough and Bent, 1998). Homozygous lines were selected in T3 generation and used for further experiments.

Real-time quantitative RT-PCR

The primer pairs used for conformation of *PLC3* (At4g38530) expression level were: 5'-TCCAGATTTCTTCGTCAAGATTGGA-3' (forward) and 5'-TATAGGAAACCACTGATCGACAGC-3' (reverse). 1μg total RNA from 10-day-old seedlings was used for cDNA synthesis as described before. Q-PCR was performed with ABI 7500 Real-Time PCR System (Applied Biosystem). The relative gene expression was determined by comparative threshold cycle value. Transcript levels were normalized by the level of *SAND* (At2g28390; forward primer: 5'-AAC TCT ATG CAG CAT TTG ATC CAC T-3', reverse primer: 5'-TGA TTG CAT ATC TTT ATC GCC ATC-3') (Han *et al.*, 2013). Three biological replicates and two technical replicates were used for the values of means and standard deviations.

Histochemical analyses for GUS activity

GUS staining was performed according to the method described by Jefferson *et al*. (1987) with minor modifications. Transgenic plants carrying *PLC3*$_{pro}$*:GUSYFP* were grown for indicated times and specific tissues were taken and incubated in X-Gluc reaction solution containing 1mg/ml 5-bromo-4-chloro-3 indolyl-β-D-glucuronic acid (X-gluc), 50 mM phosphate buffer pH 7.0 and 0.1% TX-100. The materials were incubated overnight at 37°C. The next day, the solution was replaced by 70% ethanol to destain the tissue. Plant tissues were viewed under a stereo microscope (Leica MZFLIII) and photographed (ThorLabs CCD camera).

Confocal microscopy

Arabidopsis *PLC3*$_{pro}$*:GUSYFP* seedlings were grown 5 days and then transferred to object slides containing a fixed cover slide, separated by a spacer of approximately 0.32 mm. This allows seedlings to grow in liquid medium (½ MS and 1% sucrose, pH 5.8) for 1-2 days and could directly be used for microscopy. Microscopy was performed using a Zeiss LSM 510 CLSM (confocal laser scanning microscope) (Carl-Zeiss GMBH, Jena, Germany), implemented on an inverted microscope (Axiovert 100, Carl-Zeiss GMBH, Jena, Germany). For imaging YFP, we used confocal configurations as described before (Vermeer *et al.*, 2006).

Seed germination

Mature seeds were harvested and stored at room temperature. Seeds were surface sterilized in a desiccator by using 20 ml thin bleach and 1ml 37% HCl for 3 hours and then were sown on square petri dish containing 30 ml medium consisting of ½ Murashi-Skoog (½ MS), 0.5% sucrose, pH 5.8, and 1.2 % daishin agar with or without ABA or GA at indicated concentrations under 4 °C in dark for two nights and transferred to long day condition (22 °C, 16 h of light and 8h of dark). Germination was scored as radical emergence at indicated time points by using a binocular microscope (Leica MZFLIII).

Root growth

Seeds were sterilized and stratified as described above. Plates were transfer to long day condition and placed vertically under an angle of 70°. Four-day-old seedlings with comparable size were transfer to ½ MS ager plate. The plates were scanned 12 days after germination (Epson Perfection V700 scanner). Primary root length and lateral root number from each genotype were quantified by ImageJ analysis software (National Institute of Health (NIH)). Lateral root density was expressed as the lateral number per primary length (LR number/ PR length). For gravitropic responses, seedlings were grown on ½MS plates with 0.5% sucrose for 4 days. Plates were then rotated by 90°and scanned 2 days later. Bending was expressed as curvature angle, which was quantified by imageJ analysis software (NIH) (Perera *et al*., 2006).

Stomatal aperture

The stomatal aperture measurement was performed according to Distéfano *et al*. (2012) with minor changes. The stomatal aperture treatments were performed on epidermal strips excised from the abaxial side of fully expanded Arabidopsis leaves. Epidermal peels from leaves of 3-week-old plants grown at 22°C under 16 h of light and 8h of dark were stripped and immediately floated in opening buffer (5 mM MES-KOH, pH 6.1, and 50 mM KCl) for 3 h. The strips were subsequently maintained in the same opening buffer and exposed to different ABA concentration. After 90 min, stomata were digitized using a Nikon DS-Fi 1 camera coupled to a Nikon Eclipse Ti microscope. The stomatal aperture width was measured using ImageJ software (NIH).

^{32}Pi-phospholipid labelling, extraction and analysis

Different types of tissues were labelled. For germinating seeds: Seeds were sterilized and stratified on ½ MS (pH 5.8) as described and germinated under long day condition for around 20h when testa ruptured. Germinating seeds were then transferred to 200 µl buffer (2.5 mM MES, pH 5.8, 1 mM KCl) containing 5-10 µCi $^{32}PO_4^{3-}$ ($^{32}P_i$) (carrier free; Perklin-Elmer) in 2 ml Eppendorf microcentrifuge tube for 24 h. Samples were then treated with 200 µl buffer with or without ABA for the times and concentrations indicated.

Epidermal leaf peels: Leaves of 3-week-old plants grown at 22°C under 16 h of light and 8 h of dark were stripped and immediately floated on 100 µl opening buffer (10 mM MES, pH 6.1 and 50 mM KCl) containing $^{32}P_i$ (5-10 µCi) in a 48-wells cell culture plate (Greiner bio-one) for 3 h. Samples were treated with 400 µl buffer (10 mM MES-KOH, pH 6.1, 2.5 µM $CaCl_2$) with or without ABA for the times and concentrations indicated.

Seedlings: Five-day-old seedlings were transferred to 200 µl labeling buffer (2.5 mM MES-KOH, pH 5.8, 1 mM KCl) containing $^{32}P_i$ (5-10 µCi) in 2 ml Eppendorf tubes and labeled overnight

(~16 h) or 3h. Samples were treated the next day by adding 200 µl labeling buffer with or without ABA or Sorbitol for times and concentrations indicated.

All treatments were stopped by adding perchloric acid at a final concentration of 5% (v/v) for 5-10 min, after which the material was transferred to 400 µl of $CHCl_3$/MeOH/HCl [50:100:1 v/v)] to extract the lipids. After 15 min, 400 µl of $CHCl_3$ was added followed by 200 µl of 0.9 % (w/v) NaCl to separate the extract into two phases. Lipid fractions were washed and concentrated as described earlier (Munnik & Zarza, 2013). Lipids were separated by thin-layer chromatography (TLC) using an alkaline solvent system, containing: chloroform/methanol/28% ammonia/water [90:70:4:16 (v/v)] (Munnik *et al*., 1994). Radioactive phospholipids were visualized by autoradiography and quantified by phosphoimaging (Molecular Dynamics, Sunnyvale, CA, USA). Individual phospholipid levels are expressed as the percentage of the total ^{32}P-lipid fraction.

Inositol phosphates labeling, extraction and HPLC Analyses

For the measurement of inositol polyphosphates (IPPs), two different procedures were followed. The first is based on the method described in Laha *et al.* (2015) with minor modifications. Seedlings were grown under short day (22 °C, 12 h of light and 12h of dark) and sterile conditions in plant media (½ MS, 2% sucrose, pH 5.7, 0.6% phytagel) for 11 days and then 10 seedlings were transferred to 2ml liquid medium (¼ MS, pH 5.7, 0.3% phytagel) containing ^{3}H-*myo*-inositol (80 µCi, Biotrend, ART-0261-5, Cologne, Germany) for 7 days. Seedlings were washed two times with water before harvesting and then snap-freezed into liquid N_2. IPPs were extracted (Azevedo and Saiardi, 2006) and resolved by strong anion exchange chromatography HPLC (using the partisphere SAX 4.6 x 125mm column; Whatman) at a flow rate of 0.5 mL/ min, using a shallow gradient formed by buffer A (1 mM EDTA) and buffer B (1 mM EDTA and 1.3 M Ammonium Phosphate, pH 3.8 with H_3PO_4). Fractions were collected every minute and radioactivity quantified by liquid scintillation counting. The results are expressed as percentage of total. The latter was determined by counting all fractions from 13 min to the end of the run.

Alternatively, IPP were determined as described by Desai *et al*., (2014) with some modifications. Seedlings were grown in ½ MS with 0.8 % agar under long day condition (100 µE light with a 16 h day and 8 h night cycle) for 4 days. Fifteen seedlings were incubated with 50 µl medium (1x MS, 1% sucrose, pH 5.7) and 100 µl of aqueous *myo* [2-^{3}H(N)]-inositol (100 µCi, American Radiolabeled Chemicals Cat. #ART 0116A, specific activity 20 Ci/mmol) was added to each tube. The tubes were incubated with supplemental light for 4 days. IPPs were extracted as Azevedo and Saiardi (2006) described, by vortexing the tissue with glass beads in extraction buffer (25 mM EDTA, 10 mg/ml IP_6 and 1M $HClO_4$). Samples were then neutralized to ~pH 6 to 8 with 250 mM EDTA, 1M K_2CO_3. Samples were dried to a volume of 70 µl and separated using a binary HPLC pump (Beckman Coulter) equipped with a Partisphere-SAX (4.6 x 125 mm) column, which was connected to a guard cartridge. The elution gradient was set up as described by Azevedo and Saiardi (2006) using the same

buffers as above at a flow rate of 1ml/min. An on-line IN/US radiation detector was used to generate chromatograms. Four ml of Ultima-Flo AP scintillation cocktail (Perkin Elmer, Waltham, MA, USA) was added to each 1 ml eluted fraction post-detector to quantify the radioactivity of the eluted fractions using the ^{3}H window of a Beckman Coulter LS6500 Scintillation Counter. Scintillation counts were graphed using MicroSoft Excel. The ^{3}H-*myo*-Ins cpm incorporated into total IPPs was calculated by taking the sum of cpm of all fractions and subtracting the peak of free ^{3}H-Ins cpm. The amount of each IPP was calculated as follows: [(Σ cpms in peak) / (total IPP)]*100].

Thesis for printing.docx**Drought tolerance assays**

Determination of survival rates, fresh weight (FW) and dry weight (DW) under water deficit condition and water loss were performed as described previously (Hua *et al.*, 2012; Osakabe *et al.*, 2013) with some changes. Seeds were stratified under 4°C, dark for 2 nights and sown on soil pot (4.5 cm x 4.5 cm x 7.5 cm) directly. Nine plants were grown in each pot with certain amount of soil (80 g) under short day condition (22 °C with 12 h light/12 h dark) for 4 weeks and then subjected to dehydration by withholding them for water for 2 weeks, while control plants were normally watered. And then plants were photographed. The plants were re-watered for another week and photographed. The surviving green plants were counted and survival rate was determined by the percentage of green plants compared to total plants. Each experiment used 36 plants per genotype and experiments were repeated at least 3 times.

To determine the FW and DW under dehydration stress, plants were grown under short day conditions as described above for 4 weeks and experienced 1 week dehydration by water withholding, while control plants were normally watered. Rosettes FWs were scored immediately after detachment. After complete drying, dry DWs were also determined. Eigtheen plants from each genotype were used for measurement and experiments were repeated for 3 times.

To assay the water-loss, rosettes from 4-week-old plants were detached and FW determined every one hour by weighing. Water content was calculated as a percentage from the initial FW. Twenty plants were used for each experiment and each experiment was repeated at least 3 times.

Soluble carbohydrates measurement in seeds

Soluble carbohydrates were determined as described by (Ribeiro *et al.*, 2014) with minor modifications. Three milligrams of dry seeds were transferred to a 2 mL Eppendorf tube and homogenized in 1 mL of methanol (80% v/v) with the addition of 40 µg of melezitose as internal standard. Samples were incubated in a water bath for 15 minutes at 76°C and dried by vacuum centrifugation. Then, 500 µL of milliQ water was added, thoroughly vortexed and centrifuged for 5 min at 17.000 g in an Eppendorf centrifuge. The supernatant was analyzed with a Dionex HPLC system (ICS 5000 + DC) using a CarboPac PA1, 4 x 250-mm column (Dionex) preceded by a guard column (CarboPac PA1, 4 × 50 mm). Mono-, di-, and trisaccharides were separated by elution in an increasing concentration of NaOH (20-350 mM) with a flow rate of 1 mL per minute. Peaks were identified by coelution of standards.

Phloem sap soluble carbohydrates measurement

Phloem exudates were extracted and analyzed as described earlier (Guelette *et al*., 2012; Tetyuk *et al*, 2013; modified from Roessner *et al*., 2000). The hydrophilic fraction (sugars, amino acids, small molecules) was dried and derivatized using methoxyamine in pyridine and BSTFA (N,O-bis-trimethyl-silyltrifluoroacetamide) with 1% trimethylchlorosilane. The metabolites were subsequently separated using an Agilent 5890N GC system, coupled to a 5973 inert MSD using a DB-5MS column (J&W Scientific, 30m x 0.32mm ID x 0.25 µm film; temperature program: 70-5, 5/min-320-5). Identification of compounds occurred using the NIST library (NIST Standard Reference Database; https://www.nist.gov/srd/nist-standard-reference-database-1a-v14) in combination with co-elution of standards. Peak area determination was performed using QuanLynx, a quantification software within the MassLynx software (Waters). The experiment was repeated five times.

ACKNOWLEDGEMENTS

We thank Max van Hooren for critically reading this manuscript. This work was financially supported by a grant from the China Scholarship Council (CSC File No. 201206300058 to Q.Z.) and by the Netherlands Organization for Scientific Research (NWO/ALW 813.06.003, 864.05.001, and 867.15.020 to T.M.).

REFERENCES

Allen GJ, and Sanders D (1994) Osmotic stress enhances the competence of Beta vulgaris vacuoles to respond to inositol 1,4,5-trisphosphate. *Plant J* **6**:687–695.

Arisz SA, Testerink C, and Munnik T (2009) Plant PA signaling via diacylglycerol kinase. *Biochim Biophys Acta* **1791**:869–875.

Arisz SA, van Wijk R, Roels W, Zhu JK, Haring MA, and Munnik T (2013) Rapid phosphatidic acid accumulation in response to low temperature stress in Arabidopsis is generated through diacylglycerol kinase. *Front Plant Sci* **4**:1–15.

Assmann SM, and Jegla T (2016) Guard cell sensory systems: recent insights on stomatal responses to light, abscisic acid, and CO2. *Curr Opin Plant Biol* **33**:157–167.

Balla T (2013) Phosphoinositides: tiny lipids with giant impact on cell regulation. *Physiol Rev* **93**:1019–1137.

Benková E, and Bielach A (2010) Lateral root organogenesis - from cell to organ. *Curr Opin Plant Biol* **13**:677–683.

Blatt MR (2000) Cellular signaling and volume control in stomatal movements in plants. *Annu Rev Cell Dev Biol* **16**:221–241.

Blatt MR, Thiel G, and Trentham DR (1990) Reversible inactivation of K+ channels of Vicia stomatal guard cells following the photolysis of caged inositol 1,4,5-trisphosphate. *Nature* **346**:766–769.

Boss WF, Sederoff HW, Im YJ, Moran N, Grunden AM, and Perera IY (2010) Basal Signaling Regulates Plant Growth and Development. *Plant Physiol* **154**:439–443.

Burton A, Hu X, and Saiardi A (2009) Are inositol pyrophosphates signalling molecules? *J Cell Physiol* **220**:8–15.

Chen X, Chang M, Wang B, and Wu B (1997) Cloning of a Ca2+-ATPase gene and the role of cytosolic Ca2+ in the gibberellin-dependent signaling pathway in aleurone cells. *Plant J* **11**:363–371.

Cho MH, Shears SB, and Boss WF (1993) Changes in phosphatidylinositol metabolism in response to hyperosmotic stress in Daucus carota L. cells grown in suspension culture. *Plant Physiol* **103**:637–647.

Clough SJ, and Bent AF (1998) Floral dip: A simplified method for Agrobacterium-mediated transformation of Arabidopsis thaliana. *Plant J* **16**:735–743.

Darwish E, Testerink C, Khalil M, El-Shihy O, and Munnik T (2009) Phospholipid signaling responses in salt-stressed rice leaves. *Plant Cell Physiol* **50**:986–997.

Das S, Hussain A, Bock C, Keller WA, and Georges F (2005) Cloning of Brassica napus phospholipase C2 (BnPLC2), phosphatidylinositol 3-kinase (BnVPS34) and phosphatidylinositol synthase1 (BnPtdIns S1) - Comparative analysis of the effect of abiotic stresses on the expression of phosphatidylinositol signal transdu. *Planta* **220**:777–784.

De Jong CF, Laxalt AM, Bargmann BOR, De Wit PJGM, Joosten MHAJ, and Munnik T (2004) Phosphatidic acid accumulation is an early response in the Cf-4/Avr4 interaction. *Plant J* **39**:1–12.

Desai M, Rangarajan P, Donahue JL, Williams SP, Land ES, Mandal MK, Phillippy BQ, Perera IY, Raboy V, and Gillaspy GE (2014) Two inositol hexakisphosphate kinases drive inositol pyrophosphate synthesis in plants. *Plant J* **80**:642–653.

DeWald DB, Torabinejad J, Jones C a, Shope JC, Cangelosi a R, Thompson JE, Prestwich GD, and Hama H (2001) Rapid accumulation of phosphatidylinositol 4,5-bisphosphate and inositol 1,4,5-trisphosphate correlates with calcium mobilization in salt-stressed arabidopsis. *Plant Physiol* **126**:759–769.

Di Fino L, D'Ambrosio J, Tejos R, van Wijk R, Lamattina T, Munnik T, Pagnussat G, and Laxalt AM (2017) Arabidopsis phosphatidylinositol-phospholipase C2 (PLC2) is involved in female gametogenesis and embryo development. *Planta* **2**:1–12.

Dietrich P, Sanders D, and Hedrich R (2001) The role of ion channels in light-dependent stomatal opening. *J Exp Bot* **52**:1959–1967.

Distéfano AM, Scuffi D, García-Mata C, Lamattina L, and Laxalt AM (2012) Phospholipase D?? is involved in nitric oxide-induced stomatal closure. *Planta* **236**:1899–1907.

Ditengou FA, Teale WD, Kochersperger P, Flittner KA, Kneuper I, van der Graaff E, Nziengui H, Pinosa F, Li X, Nitschke R, Laux T, and Palme K (2008) Mechanical induction of lateral root initiation in Arabidopsis thaliana. *Proc Natl Acad Sci U S A* **105**:18818–18823.

Dowd PE, Coursol S, Skirpan AL, Kao T, and Gilroy S (2006) Petunia phospholipase C1 is involved in pollen tube growth. *Plant Cell* **18**:1438–1453.

Fleet CM, Ercetin ME, and Gillaspy GE (2009) Inositol phosphate signaling and gibberellic acid. *Plant Signal Behav* **4**:73–74.

Flores S, and Smart CC (2000) Abscisic acid-induced changes in inositol metabolism in Spirodela polyrrhiza. *Planta* **211**:823–832.

Gangl R, and Tenhaken R (2016) Raffinose family oligosaccharides act as galactose stores in seeds and are required for rapid germination of Arabidopsis in the Dark. *Front Plant Sci* **7**:1–15.

Gao K, Liu YL, Li B, Zhou RG, Sun DY, and Zheng SZ (2014) Arabidopsis thaliana phosphoinositide-specific phospholipase C isoform 3 (AtPLC3) and AtPLC9 have an additive effect on thermotolerance. *Plant Cell Physiol* **55**:1873–1883.

Georges F, Das S, Ray H, Bock C, Nokhrina K, Kolla VA, and Keller W (2009) Over-expression of Brassica napus phosphatidylinositol-phospholipase C2 in canola induces significant changes in gene expression and phytohormone distribution patterns, enhances drought tolerance and promotes early flowering and maturation. *Plant, Cell Environ* **32**:1664–1681.

Gillaspy GE (2011) The cellular language of myo-inositol signaling. *New Phytol* **192**:823–839.

Gillaspy GE (2013) The role of phosphoinositides and inositol phosphates in plant cell signaling, in *Lipid-mediated protein signaling* (Capelluto DGS ed) pp 141–157.

Gilroy S, Read ND, and Trewavas a J (1990) Elevation of cytoplasmic calcium by caged calcium or caged inositol triphosphate initiates stomatal closure. *Nature* **346**:769–771.

Gonorazky G, Guzzo MC, and Laxalt AM (2016) Silencing of the tomato phosphatidylinositol-phospholipase C2 (SlPLC2) reduces plant susceptibility to Botrytis cinerea. *Mol Plant Pathol* **2**:1–10.

Gonorazky G, Ramirez L, Abd-El-Haliem A, Vossen JH, Lamattina L, ten Have A, Joosten MHAJ, and Laxalt AM (2014) The tomato phosphatidylinositol-phospholipase C2 (SlPLC2) is required for defense gene induction by the fungal elicitor xylanase. *J Plant Physiol* **171**:959–965.

Han B, Yang Z, Samma MK, Wang R, and Shen W (2013) Systematic validation of candidate reference genes for qRT-PCR normalization under iron deficiency in Arabidopsis. *BioMetals* **26**:403–413.

Hartog M Den, Verhoef N, and Munnik T (2003) Nod factor and elicitors activate different phospholipid signaling pathways in suspension-cultured Alfalfa cells. *Plant Physiol* **132**:311–317.

Heilmann I (2016) Phosphoinositide signaling in plant development. *Development* **143**:2044–2055.

Helling D, Possart A, Cottier S, Klahre U, and Kost B (2006) Pollen tube tip growth depends on plasma membrane polarization mediated by tobacco PLC3 activity and endocytic membrane recycling. *Plant Cell* **18**:3519–3534.

Hirayama T, Ohtot C, Mizoguchi T, and Shinozaki K (1995) A gene encoding a phosphatidylinositol-specific phospholipase C is induced by dehydration and salt stress in Arabidopsis thaliana. *Proc Natl Acad Sci USA* **92**:3903–3907.

Hirayama T, and Umezawa T (2010) The PP2C–SnRK2 complex. *Plant Signal Behav* **5**:160–163.

Horvath I, Glatz A, Nakamoto H, Mishkind ML, Munnik T, Saidi Y, Goloubinoff P, Harwood JL, and Vigh L (2012) Heat shock response in photosynthetic organisms: Membrane and lipid connections. *Prog Lipid Res* **51**:208–220.

Hou Q, Ufer G, and Bartels D (2016) Lipid signalling in plant responses to abiotic stress. *Plant, Cell Environ* **39**:1029–1048.

Hua D, Wang C, He J, Liao H, Duan Y, Zhu Z, Guo Y, Chen Z, and Gong Z (2012) A plasma membrane receptor kinase, GHR1, mediates abscisic acid- and hydrogen peroxide-regulated stomatal movement in Arabidopsis. *Plant Cell* **24**:2546–61.

Hunt L, and Gray JE (2001) ABA signalling: A messenger's FIERY fate. *Curr Biol* **11**:968–970.

Hunt L, Mills LN, Pical C, Leckie CP, Aitken FL, Kopka J, Mueller-Roeber B, McAinsh MR, Hetherington AM, and Gray JE (2003) Phospholipase C is required for the control of stomatal aperture by ABA. *Plant J* **34**:47–55.

Hunt L, Otterhag L, Lee JC, Lasheen T, Hunt J, Seki M, Shinozaki K, Sommarin M, Gilmour DJ, Pical C, and Gray JE (2004) Gene-specific expression and calcium activation of Arabidopsis thaliana phospholipase C isoforms. *New Phytol* **162**:643–654.

Irvine RF (2006) Nuclear inositide signalling-expansion, structures and clarification. *Biochim Biophys Acta* **1761**:505–508.

Jefferson RA, Kavanagh TA, and Bevan MW (1987) GUS fusions: beta-glucuronidase as a sensitive and versatile gene fusion marker in higher plants. *EMBO J* **6**:3901–3907.

Kashem M, Itoh K, Iwabuchi S, Hori H, and Mitsui T (2000) Possible involvement of phosphoinositide-Ca2+ signaling in the regulation of alpha-amylase expression and germination of rice seed (Oryza sativa L.). *Plant cell Physiol* **41**:399–407.

Kepinski S, and Leyser O (2005) The Arabidopsis F-box protein TIR1 is an auxin receptor. *Nature* **435**:446–451.

Kulik A, Wawer I, Krzywińska E, Bucholc M, and Dobrowolska G (2011) SnRK2 protein kinases—key regulators of plant

response to abiotic stresses. *Omi A J Integr Biol* **15**:859–872.
Laha D, Johnen P, Azevedo C, Dynowski M, Weiß M, Capolicchio S, Mao H, Iven T, Steenbergen M, Freyer M, Gaugler P, de Campos MKF, Zheng N, Feussner I, Jessen HJ, Van Wees SCM, Saiardi A, and Schaaf G (2015) VIH2 regulates the synthesis of inositol pyrophosphate InsP8 and jasmonate-dependent defenses in Arabidopsis. *Plant Cell* **27**:1082–1097.
Laha D, Parvin N, Dynowski M, Johnen P, Mao H, Bitters ST, Zheng N, and Schaaf G (2016) Inositol polyphosphate binding specificity of the jasmonate receptor complex. *Plant Physiol* **171**:2364–2370.
Lanteri ML, Lamattina L, and Laxalt AM (2011) Mechanisms of xylanase-induced nitric oxide and phosphatidic acid production in tomato cells. *Planta* **234**:845–855.
Laxalt AM, and Munnik T (2002) Phospholipid signalling in plant defence. *Curr Opin Plant Biol* **5**:332–338.
Lee Y, Choi YB, Suh S, Lee J, Assmann SM, Joe CO, Kelleher JF, and Crain RC (1996) Abscisic acid-induced phosphoinositide turnover in guard cell protoplasts of Vicia faba. *Plant Physiol* **110**:987–996.
Lee Y, Kim YW, Jeon BW, Park KY, Suh SJ, Seo J, Kwak JM, Martinoia E, Hwang I, and Lee Y (2007) Phosphatidylinositol 4,5-bisphosphate is important for stomatal opening. *Plant J* **52**:803–816.
Lemtiri-Chlieh F, MacRobbie EAC, and Brearley CA (2000) Inositol hexakisphosphate is a physiological signal regulating the K^+-inward rectifying conductance in guard cells. *Proc Natl Acad Sci U S A* **97**:8687–8692.
Lemtiri-Chlieh F, MacRobbie EAC, Webb AAR, Manison NF, Brownlee C, Skepper JN, Chen J, Prestwich GD, and Brearley CA (2003) Inositol hexakisphosphate mobilizes an endomembrane store of calcium in guard cells. *Proc Natl Acad Sci U S A* **100**:10091–10095.
Li L, He Y, Wang Y, Zhao S, Chen X, Ye T, Wu Y, and Wu Y (2015) Arabidopsis PLC2 is involved in auxin-modulated reproductive development. *Plant J* **84**:504–515.
Lin WH, Ye R, Ma H, Xu ZH, and Xue HW (2004) DNA chip-based expression profile analysis indicates involvement of the phosphatidylinositol signaling pathway in multiple plant responses to hormone and abiotic treatments. *Cell Res* **14**:34–45.
Liu HT, Huang WD, Pan QH, Weng FH, Zhan JC, Liu Y, Wan SB, and Liu YY (2006) Contributions of PIP2-specific-phospholipase C and free salicylic acid to heat acclimation-induced thermotolerance in pea leaves. *J Plant Physiol* **163**:405–416.
Liu HT, Liu YY, Pan QH, Yang HR, Zhan JC, and Huang WD (2006) Novel interrelationship between salicylic acid, abscisic acid, and PIP 2-specific phospholipase C in heat acclimation-induced thermotolerance in pea leaves. *J Exp Bot* **57**:3337–3347.
Luit AH Van Der, Piatti T, Doorn A Van, Musgrave A, Felix G, Boller T, and Munnik T (2000) Elicitation of Suspension-Cultured Tomato Cells Triggers the Formation of Phosphatidic Acid and Diacylglycerol Pyrophosphate 1. *Plant Physiol* **123**:1507–1515.
Luo Y, Xie W, and Luo F (2012) Effect of several germination treatments on phosphatases activities and degradation of phytate in Faba Bean (Vicia faba L.) and Azuki Bean (Vigna angularis L.). *J Food Sci* **77**:1023–1029.
Ma Y, Szostkiewicz I, Korte A, Moes D, Yang Y, Christmann A, and Grill E (2009) Regulators of PP2C phosphatase activity function as abscisic acid sensors. *Science* **324**:1064–1069.
Martin TF. (2001) PI(4,5)P2 regulation of surface membrane traffic. *Curr Opin Cell Biol* **13**:493–499.
Meijer HJG, and Munnik T (2003) Phospholipid-based signaling in plants. *Annu Rev Plant Biol* **54**:265–306.
Melcher K, Ng L-M, Zhou XE, Soon F-F, Xu Y, Suino-Powell KM, Park S-Y, Weiner JJ, Fujii H, Chinnusamy V, Kovach A, Li J, Wang Y, Li J, Peterson FC, Jensen DR, Yong E-L, Volkman BF, Cutler SR, Zhu J-K, and Xu HE (2009) A gate-latch-lock mechanism for hormone signalling by abscisic acid receptors. *Nature* **462**:602–608, Nature Publishing Group.
Michell RH (2008) Inositol derivatives: evolution and functions. *Nat Rev* **9**:151–161.
Mickelbart M V., Hasegawa PM, and Bailey-Serres J (2015) Genetic mechanisms of abiotic stress tolerance that translate to crop yield stability. *Nat Rev Genet* **16**:237–251.
Mills LN, Hunt L, Leckie CP, Aitken FL, Wentworth M, McAinsh MR, Gray JE, and Hetherington AM (2004) The effects of manipulating phospholipase C on guard cell ABA-signalling. *J Exp Bot* **55**:199–204.
Mishkind M, Vermeer JEM, Darwish E, and Munnik T (2009) Heat stress activates phospholipase D and triggers PIP accumulation at the plasma membrane and nucleus. *Plant J* **60**:10–21.
Miyazono K-I, Miyakawa T, Sawano Y, Kubota K, Kang H-J, Asano A, Miyauchi Y, Takahashi M, Zhi Y, Fujita Y, Yoshida T, Kodaira K-S, Yamaguchi-Shinozaki K, and Tanokura M (2009) Structural basis of abscisic acid signalling. *Nature* **462**:609–614, Nature Publishing Group.
Mueller-roeber B, and Pical C (2002) Inositol phospholipid metabolism in Arabidopsis . characterized and putative isoforms of inositol phospholipid kinase and phosphoinositide-specific phospholipase C. *Plant Physiol* **130**:22–46.
Munemasa S, Hauser F, Park J, Waadt R, Brandt B, and Schroeder JI (2015) Mechanisms of abscisic acid-mediated control of stomatal aperture. *Curr Opin Plant Biol* **28**:154–162.
Munnik T (2001) Phosphatidic acid: an emerging plant lipid second messenger. *Trends Plant Sci* **6**:227–233.
Munnik T (2014) PI-PLC: Phosphoinositide-phospholipase C in plant signalling, in *Phospholipases in Plant Signaling* (Wang X ed) pp 27–54.
Munnik T, and Laxalt A. (2013) Measuring PLD Activity In Vivo, in *Plant Lipid Signaling Protocols* (Munnik T, and Heilmann I eds) pp 219–231.
Munnik T, and Meijer HJ. (2001) Osmotic stress activates distinct lipid and MAPK signalling pathways in plants. *FEBS Lett* **498**:172–178.
Munnik T, Musgrave A, and de Vrije T (1994) Rapid turnover of polyphosphoinositides in carnation flower petals. *Planta* **193**:89–98.
Munnik T, and Nielsen E (2011) Green light for polyphosphoinositide signals in plants. *Curr Opin Plant Biol* **14**:489–497.
Munnik T, and Testerink C (2009) Plant phospholipid signaling: “in a nutshell”. *J Lipid Res* **50**:S260–S265.

Munnik T, van Himbergen JAJ, ter Riet B, Braun F-J, Irvine RF, van den Ende H, and Musgrave A (1998) Detailed analysis of the turnover of polyphosphoinositides and phosphatidic acid upon activation of phospholipases C and D in Chlamydomonas cells treated with non-permeabilizing concentrations of mastoparan. *Planta* **207**:133–145.

Munnik T, and Vermeer JEM (2010) Osmotic stress-induced phosphoinositide and inositol phosphate signalling in plants. *Plant Cell Environ* **33**:655–669.

Munnik T, and Zarza X (2013) Analyzing Plant Signaling Phospholipids Through 32Pi-Labeling and TLC, in *Plant Lipid Signaling Protocols* (Munnik T, and Heilmann I eds) pp 3–15.

Murthy PP, Renders JM, and Keranen LM (1989) Phosphoinositides in barley aleurone layers and gibberellic Acid-induced changes in metabolism. *Plant Physiol* **91**:1266–1269.

Nakashima K, and Yamaguchi-Shinozaki K (2013) ABA signaling in stress-response and seed development. *Plant Cell Rep* **32**:959–970.

Nambara E, Okamoto M, Tatematsu K, Yano R, Seo M, and Kamiya Y (2010) Abscisic acid and the control of seed dormancy and germination. *Seed Sci Res* **20**:55–67.

Nishimura N (2009) Structural mechanism of abscisic acid bind and signaling by dimeric PYR1. *Science (80-)* **326**:1373–1380.

Nokhrina K, Ray H, Bock C, and Georges F (2014) Metabolomic shifts in Brassica napus lines with enhanced BnPLC2 expression impact their response to low temperature stress and plant pathogens. *GM Crops Food* **5**:120–131.

Osakabe Y, Arinaga N, Umezawa T, Katsura S, Nagamachi K, Tanaka H, Ohiraki H, Yamada K, Seo S-U, Abo M, Yoshimura E, Shinozaki K, and Yamaguchi-Shinozaki K (2013) Osmotic stress responses and plant growth controlled by potassium transporters in Arabidopsis. *Plant Cell* **25**:609–624.

Otegui MS, Capp R, and Staehelin LA (2002) Developing seeds of Arabidopsis store different minerals in two types of vacuoles and in the endoplasmic reticulum. *Plant Cell* **14**:1311–1327.

Park S, Fung P, Nishimura N, Jensen DR, Fujii H, Zhao Y, Lumba S, Santiago J, Rodrigues A, Chow TF, Alfred SE, Bonetta D, Finkelstein R, Provart NJ, Desveaux D, Rodriguez PL, McCourt P, Zhu J-K, Schroeder JI, Volkmann BF, and Cutler SR (2014) Abscisic acid inhibits type 2C protein phosphatases via the PYR/PYL family of START proteins. *Science (80-)* **324**:1068–1069.

Perera IY, Heilmann I, and Boss WF (1999) Transient and sustained increases in inositol 1,4,5-trisphosphate precede the differential growth response in gravistimulated maize pulvini. *Proc Natl Acad Sci USA* **96**:5838–5843.

Perera IY, Hung C, Brady S, Muday GK, and Boss WF (2006) A Universal Role for Inositol 1, 4, 5-Trisphosphate-Mediated Signaling in Plant Gravitropism. *Plant Physiol* **140**:746–760.

Péret B, De Rybel B, Casimiro I, Benková E, Swarup R, Laplaze L, Beeckman T, and Bennett MJ (2009) Arabidopsis lateral root development: an emerging story. *Trends Plant Sci* **14**:399–408.

Péret B, Larrieu A, and Bennett MJ (2009) Lateral root emergence: A difficult birth. *J Exp Bot* **60**:3637–3643.

Pical C, Westergren T, Dove SK, Larsson C, and Sommarin M (1999) Salinity and hyperosmotic stress induce rapid increases in phosphatidylinositol 4,5-bisphosphate, diacylglycerol pyrophosphate, and phosphatidylcholine in Arabidopsis thaliana cells. *J Biol Chem* **274**:38232–38240.

Pieterse CMJ (1998) A novel signaling pathway controlling induced systemic resistance in Arabidopsis. *Plant Cell* **10**:1571–1580.

Pokotylo I, Kolesnikov Y, Kravets V, Zachowski A, and Ruelland E (2014) Plant phosphoinositide-dependent phospholipases C: Variations around a canonical theme. *Biochimie* **96**:144–157.

Raho N, Ramirez L, Lanteri ML, Gonorazky G, Lamattina L, ten Have A, and Laxalt AM (2011) Phosphatidic acid production in chitosan-elicited tomato cells, via both phospholipase D and phospholipase C/diacylglycerol kinase, requires nitric oxide. *J Plant Physiol* **168**:534–539.

Repp A, Mikami K, Mittmann F, and Hartmann E (2004) Phosphoinositide-specific phospholipase C is involved in cytokinin and gravity responses in the moss Physcomitrella patens. *Plant J* **40**:250–259.

Ribeiro PR, Fernandez LG, de Castro RD, Ligterink W, and Hilhorst HW (2014) Physiological and biochemical responses of Ricinus communis seedlings to different temperatures: a metabolomics approach. *BMC Plant Biol* **14**:1–14.

Rodriguez-Villalon A, Gujas B, van Wijk R, Munnik T, and Hardtke CS (2015) Primary root protophloem differentiation requires balanced phosphatidylinositol-4,5-biphosphate levels and systemically affects root branching. *Development* **142**:1437–1446.

Roelfsema MRG, Hedrich R, and Geiger D (2012) Anion channels: master switches of stress responses. *Trends Plant Sci* **17**:221–9, Elsevier Ltd.

Ruelland E, Cantrel C, Gawer M, Kader JC, and Zachowski A (2002) Activation of phospholipases C and D is an early response to a cold exposure in Arabidopsis suspension cells. *Plant Physiol* **130**:999–1007.

Sanchez JP, and Chua NH (2001) Arabidopsis PLC1 is required for secondary responses to abscisic acid signals. *Plant Cell* **13**:1143–1154.

Santiago J, Rodrigues A, Saez A, Rubio S, Antoni R, Dupeux F, Park SY, Márquez JA, Cutler SR, and Rodriguez PL (2009) Modulation of drought resistance by the abscisic acid receptor PYL5 through inhibition of clade A PP2Cs. *Plant J* **60**:575–588.

Schroeder JI, Allen GJ, Hugouvieux V, Kwak JM, and Waner D (2001) Guard cell signal transduction. *Annu Rev Plant Physiol plant mol biol* **52**:627–658.

Sean R, Pedro L, Ruth R, and Suzanne R (2010) Abscisic acid:emergence of a core signaling network. *Annu Rev Plant Biol* **61**:651–679.

Sengupta S, Mukherjee S, Basak P, and Majumder AL (2015) significance of galactinol and raffinose family oligosaccharide synthesis in plants. *Front Plant Sci* **6**:1–11.

Shears SB (2009) Diphosphoinositol polyphosphates: metabolic messengers? *Mol Pharmacol* **76**:236–252.

Siegel RS, Xue S, Murata Y, Yang Y, Nishimura N, Wang A, and Schroeder JI (2009) Calcium elevation-dependent and

attenuated resting calcium-dependent abscisic acid induction of stomatal closure and abscisic acid-induced enhancement of calcium sensitivities of S-type anion and inward-rectifying K channels in Arabidopsis guard cells. *Plant J* **59**:207–220.

Song M, Liu S, Zhou Z, and Han Y (2008) TfPLC1, a gene encoding phosphoinositide-specific phospholipase C, is predominantly expressed in reproductive organs in Torenia fournieri. *Sex Plant Reprod* **21**:259–267.

Soon F-F, Ng L-M, Zhou XE, West GM, Kovach A., Tan MHE, Suino-Powell KM, He Y, Xu Y, Chalmers MJ, Brunzelle JS, Zhang H, Yang H, Jiang H, Li J, Yong E-L, Cutler S, Zhu J-K, Griffin PR, Melcher K, and Xu HE (2012) Molecular Mimicry Regulates ABA Signaling by SnRK2 Kinases and PP2C Phosphatases. *Science (80-)* **335**:85–88.

Staxen I, Pical C, Montgomery LT, Gray JE, Hetherington M, and McAinsh MR (1999) Abscisic acid induces oscillations in guard-cell cytosolic free calcium that involve phosphoinositide-specific phospholipase C. *Proc Natl Acad Sci U S A* **96**:1779–1784.

Stevenson-Paulik J, Bastidas RJ, Chiou S-T, Frye R a, and York JD (2005) Generation of phytate-free seeds in Arabidopsis through disruption of inositol polyphosphate kinases. *Proc Natl Acad Sci U S A* **102**:12612–12617.

Stevenson JM, Perera IY, Heilmann I, Persson S, and Boss WF (2000) Inositol signaling and plant growth. *Trends Plant Sci* **5**:252–258.

Sui Z, Niu L, Yue G, Yang A, and Zhang J (2008) Cloning and expression analysis of some genes involved in the phosphoinositide and phospholipid signaling pathways from maize (Zea mays L.). *Gene* **426**:47–56.

Takahashi S, Katagiri T, Hirayama T, Yamaguchi-Shinozaki K, and Shinozaki K (2001) Hyperosmotic stress induces a rapid and transient increase in inositol 1,4,5-trisphosphate independent of abscisic acid in Arabidopsis cell culture. *Plant Cell Physiol* **42**:214–222.

Tan X, Calderon-Villalobos LI a, Sharon M, Zheng C, Robinson C V, Estelle M, and Zheng N (2007) Mechanism of auxin perception by the TIR1 ubiquitin ligase. *Nature* **446**:640–645.

Tasma IM, Brendel V, Whitham S a., and Bhattacharyya MK (2008) Expression and evolution of the phosphoinositide-specific phospholipase C gene family in Arabidopsis thaliana. *Plant Physiol Biochem* **46**:627–637.

Testerink C, and Munnik T (2005) Phosphatidic acid: a multifunctional stress signaling lipid in plants. *Trends Plant Sci* **10**:368–375.

Tripathy MK, Tyagi W, Goswami M, Kaul T, Singla-Pareek SL, Deswal R, Reddy MK, and Sopory SK (2011) Characterization and Functional Validation of Tobacco PLC Delta for Abiotic Stress Tolerance. *Plant Mol Biol Report* **30**:488–497.

Valluru R, and Van den Ende W (2011) Myo-inositol and beyond - emerging networks under stress. *Plant Sci* **181**:387–400, Elsevier Ireland Ltd.

Van den Ende W (2013) Multifunctional fructans and raffinose family oligosaccharides. *Front Plant Sci* **4**:1–11.

van Leeuwen W, Vermeer JEM, Gadella TWJ, and Munnik T (2007) Visualization of phosphatidylinositol 4,5-bisphosphate in the plasma membrane of suspension-cultured tobacco BY-2 cells and whole Arabidopsis seedlings. *Plant J* **52**:1014–1026.

Vermeer JEM, Thole JM, Goedhart J, Nielsen E, Munnik T, and Gadella TWJ (2009) Imaging phosphatidylinositol 4-phosphate dynamics in living plant cells. *Plant J* **57**:356–372.

Vermeer JEM, van Leeuwen W, Tobeña-Santamaria R, Laxalt AM, Jones DR, Divecha N, Gadella TWJ, and Munnik T (2006) Visualization of PtdIns3P dynamics in living plant cells. *Plant J* **47**:687–700.

Villasuso AL, Molas ML, Racagni G, Abdala G, and Machado-Domenech E (2003) Gibberellin signal in barley aleurone: Early activation of PLC by G protein mediates amylase secretion. *Plant Growth Regul* **41**:197–205.

Vossen JH, Abd-El-Haliem A, Fradin EF, Van Den Berg GCM, Ekengren SK, Meijer HJG, Seifi A, Bai Y, Ten Have A, Munnik T, Thomma BPHJ, and Joosten MHAJ (2010) Identification of tomato phosphatidylinositol-specific phospholipase-C (PI-PLC) family members and the role of PLC4 and PLC6 in HR and disease resistance. *Plant J* **62**:224–239.

Wang CR, Yang AF, Yue GD, Gao Q, Yin HY, and Zhang JR (2008) Enhanced expression of phospholipase C 1 (ZmPLC1) improves drought tolerance in transgenic maize. *Planta* **227**:1127–1140.

Ward JM, Mäser P, and Schroeder JI (2009) Plant ion channels: gene families, physiology, and functional genomics analyses. *Annu Rev Physiol* **71**:59–82.

Wheeler GL, and Brownlee C (2008) Ca^{2+} signalling in plants and green algae - changing channels. *Trends Plant Sci* **13**:506–514.

Yin P, Fan H, Hao Q, Yuan X, Wu D, Pang Y, Yan C, Li W, Wang J, and Yan N (2009) Structural insights into the mechanism of abscisic acid signaling by PYL proteins. *Nat Struct Mol Biol* **16**:1230–1236.

York JD (2006) Regulation of nuclear processes by inositol polyphosphates. *Biochim Biophys Acta - Mol Cell Biol Lipids* **1761**:552–559.

Zarza X, Atanasov KE, Marco F, Arbona V, Carrasco P, Kopka J, Fotopoulos V, Munnik T, Gomez-Cadenas A, Tiburcio AF, and Alczar R (2016) Polyamine oxidase 5 loss-of-function mutations in Arabidopsis thaliana trigger metabolic and transcriptional reprogramming and promote salt stress tolerance. *Plant, Cell Environ* 1–16.

Zhang J, Vanneste S, Brewer PB, Michniewicz M, Grones P, Kleine-Vehn J, Löfke C, Teichmann T, Bielach A, Cannoot B, Hoyerová K, Chen X, Xue HW, Benková E, Zažímalová E, and Friml J (2011) Inositol trisphosphate-induced Ca^{2+} signaling modulates auxin transport and pin polarity. *Dev Cell* **20**:855–866.

Zheng S, Liu Y, Li B, Shang Z, Zhou R, and Sun D (2012) Phosphoinositide-specific phospholipase C9 is involved in the thermotolerance of Arabidopsis. *Plant J* **69**:689–700.

Zhu J (2016) Abiotic Stress Signaling and Responses in Plants. *Cell* **167**:313–324.

Zhu J (2002) Salt and Drought stress signal transduction in plants. *Annu Rev Plant Biol* **53**:247–273.

Zonia L, and Munnik T (2004) Osmotically induced cell swelling versus cell shrinking elicits specific changes in phospholipid signals in tobacco pollen tubes. *Plant Physiol* **134**:813–823.

SUPPLEMENTAL DATA

Supplemental Table S1. Primers for the identification of *PLC3* T-DNA insertion mutants and for *PLC3* RT-PCR.

Primers	Sequence
*PLC3*_Forward	TGCTGAAGTTCGTCATGGCAG
*PLC3*_Reverse	GTCCACCCAACATGAGGATCG
LBa*	TGGTTCACGTAGTGGGCCATCG
TUBLINα4_Forward	CCAGCCACCAACAGTTGTTC
TUBLINα4_Reverse	CACAAGACGAGATTATAGAGA

- LBa and *PLC*3_Forward combination is for T-DNA insertion identification

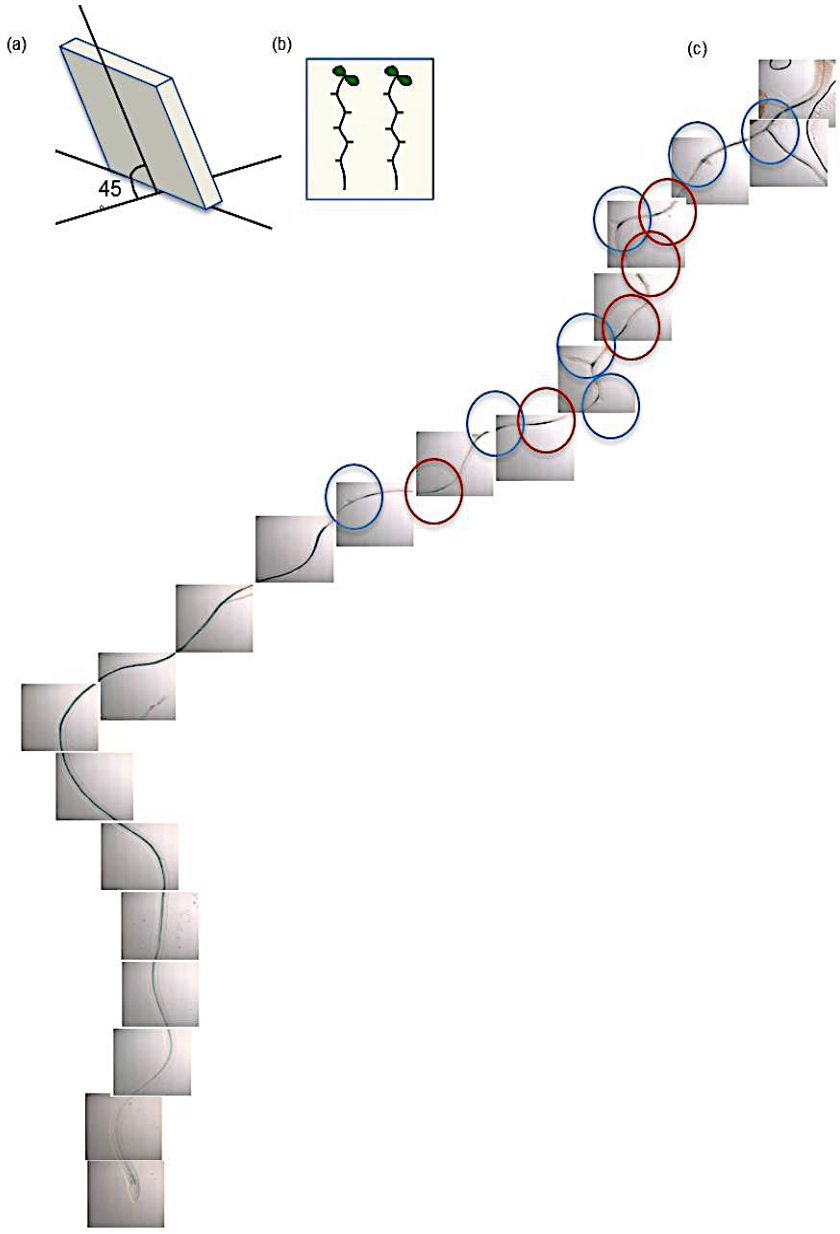

Supplemental Figure S1. *PLC3$_{pro}$:GUS-YFP* expression in seedling grown at 45° angle.
To find a stronger correlation between lateral root formation and the segmented PLC3-GUS expression, seedlings were grown on ½MS agar plates at an angle of 45° for 10 days to force later root formation at the curved sites of the primary root. (a) Cartoon of the setup. (b) Cartoon of the curvy seedlings generated and the lateral root formation at the curved sites (blue circles). (c) Histological GUS analysis of *PLC3$_{pro}$:GUS-YFP* seedlings grown for 10-d at a 45° angle. Using this setup, less segments without lateral root were found (red circles). These results also show that GUS activity is not homogenously expressed throughout the root vasculature, going from segmented (top), to complete GUS possitive (middle) to no GUS activity (root tip, transition zone).

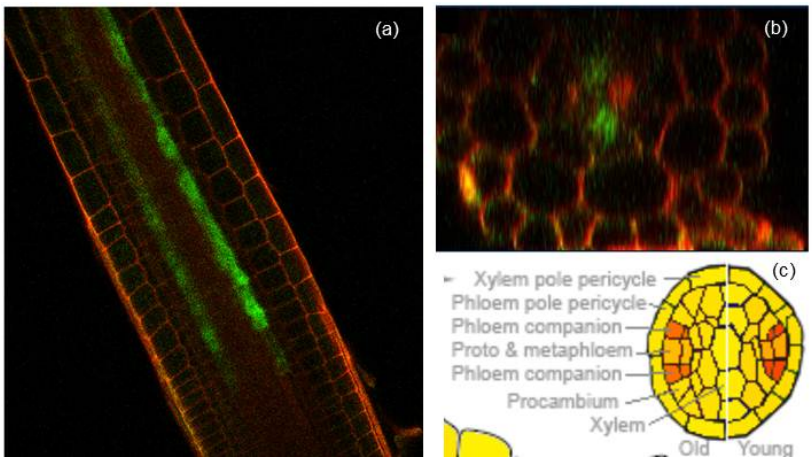

Supplemental Figure S2. Confocal analysis of *PLC3*$_{pro}$*:GUS-YFP* expression.
Confocal image of longitudinal section (a) and cross section (b) of 5-d old seedlings. (c) eFP browser database of *PLC3* expression in old and young root tissues.

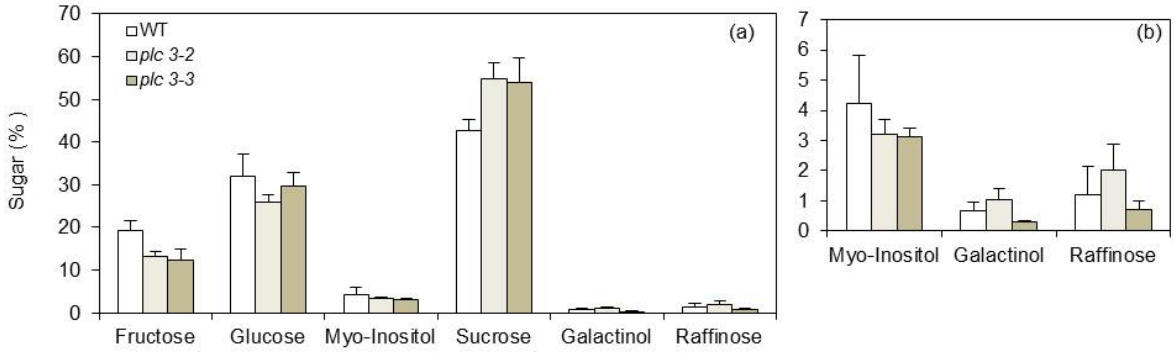

Supplemental Figure S3. Soluble carbohydrates content in the phloem sap of wild-type and *plc3* mutants.
Phloem was isolated from 6-week-old Arabidopsis plants and their carbohydrates analyzed and quantified by GC-MS . Values are the means of triplicates ± SD from 3 independent experiments.

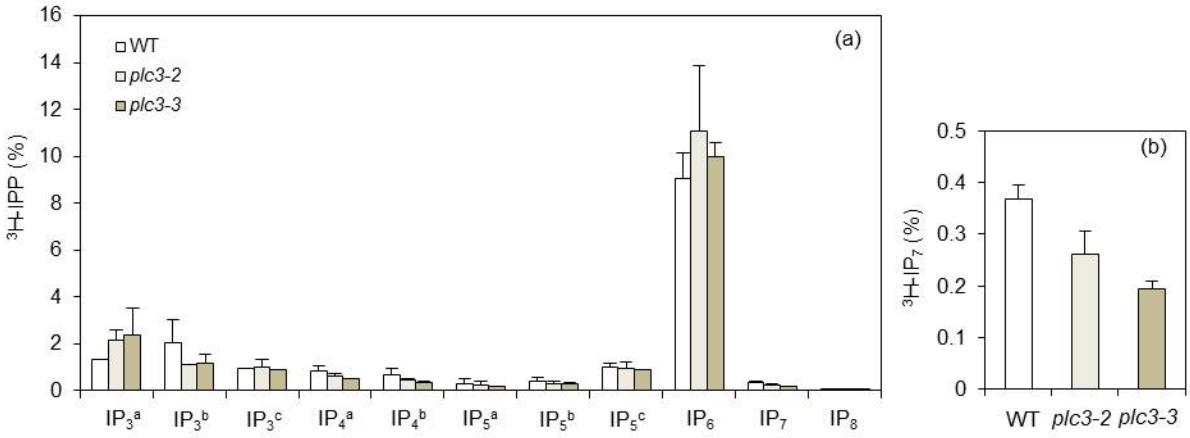

Supplemental Figure S4. Inositolpolyphosphate levels in wild-type and *plc3* mutants.
(a) Inositolpolyphosphate levels in wild-type and *plc3* mutants. (b) IP_7 in wild type and *plc3*-mutant seedlings. Four-days old seedlings were labelled with [2-^{3}H(N)]-inositol for 4 days after which IPPs were extracted and resolved by HPLC-SAX analysis. Fractions were collected each minute and analyzed by liquid scintillation counting. The ^{3}H-*myo*-Ins cpm incorporated into all inositolphosphates (total IPs) was calculated by taking the sum of cpm of all fractions and subtracting the ^{3}H-Ins peak cpm. The amount of each IP was calculated as follows: [(Σ cpms in peak) / (total InsPs)]*100]. Data shown are means ± SE (n=10) from three independent experiments.

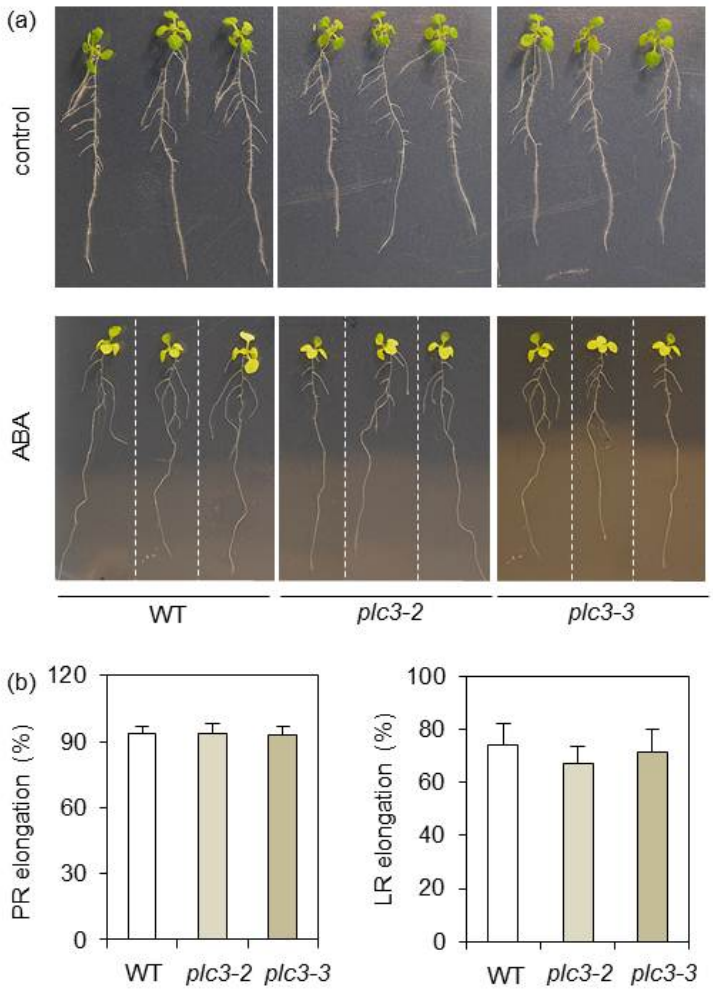

Supplemental Figure S5. Effect of ABA on root development in wild-type and *plc3* mutants.
(a) Seedling morphology of wild-type and *plc3* under normal and ABA conditions. Seeds were germinated on ½MS with 0.5% sucrose for 4 days and then transferred to ½ MS with and without ABA (10 µM). Photographs were taken 12 d after germination. (b) Relative primary root- (PR-) and lateral root (LR) growth were calculated as a percentage of the length under control condition. Three independent experiments were performed. Data shown are the means ± SD (n>10) for one representative experiment.

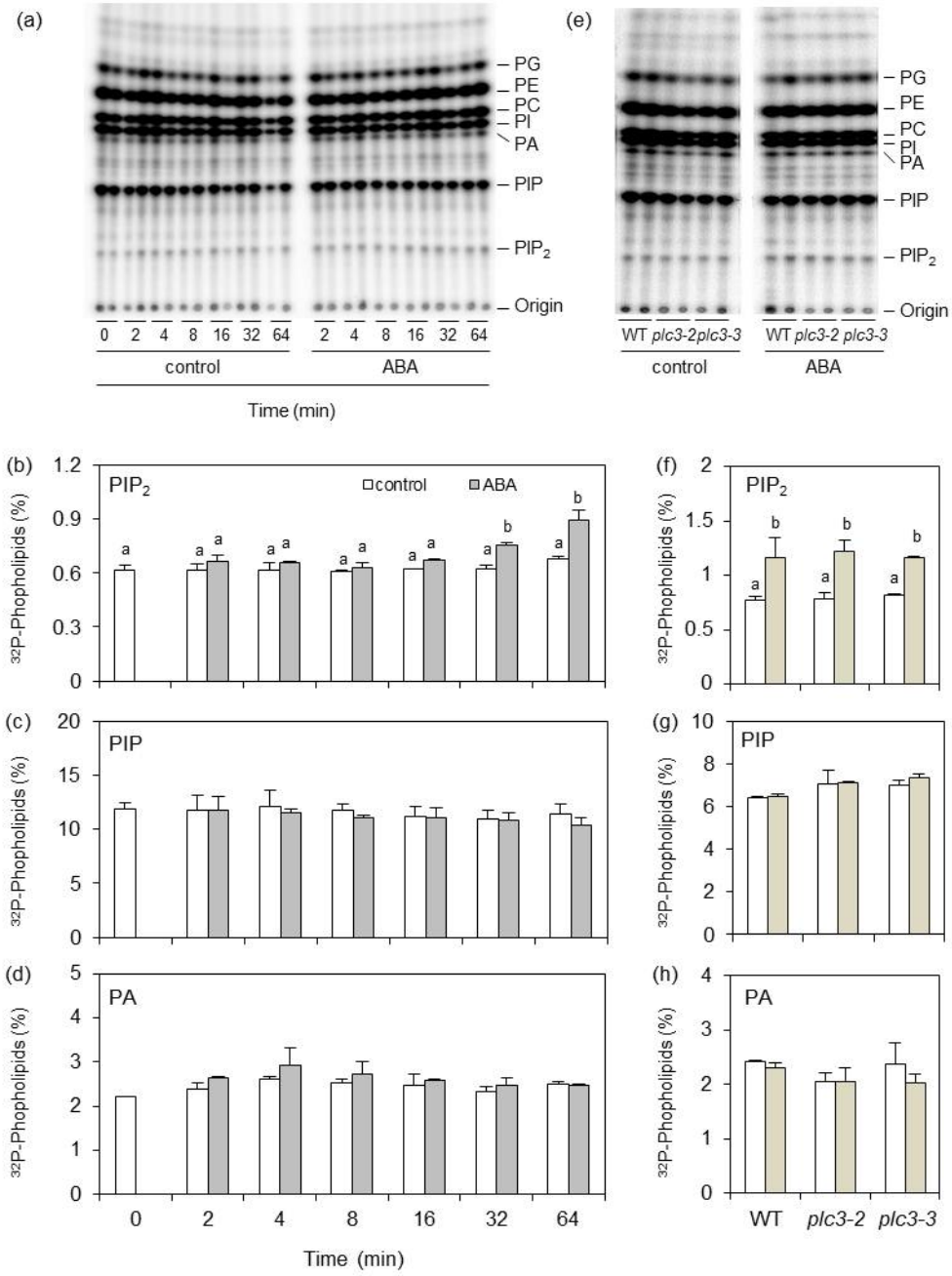

Supplemental Figure S6. Effect of ABA on phospholipid-signaling responses in *Arabidopsis* wt- and *plc3* seedlings.
(a-d) Time-course of ABA response in wt seedlings. Six-day-old seedlings were $^{32}P_i$-labeled for 3h and then treated with buffer with or without 100 µM ABA for different periods of time (0, 2, 4, 8, 16, 32 and 64 min). Lipids were extracted and separate by TLC. Radioactivity was visualized by autoradiography (a) and quantified by phosphoimaging (b-d). Lipids are expressed as fold-increase with respect to control. Values are the means of triplicates ± SD for one representative experiment. Data was analyzed by 2-way ANOVA. Statistical significant differences between genotypes are indicated by letters ($P<0.05$, Dunn's method).
(e-h) ABA response in *plc3* mutants. Five-day-old wt- and *plc3* seedlings were $^{32}P_i$-labeled for 3h and then treated with buffer or 100 µM ABA for 1 h. (e) Autoradiograph of TLC. (f-h) Quantification of PIP_2, PIP and PA. Data shown are the means ± SE of three independent experiments. Data was analyzed by 2-way ANOVA. Statistical significant differences between genotypes are indicated by letters ($P<0.05$, Dunn's method).

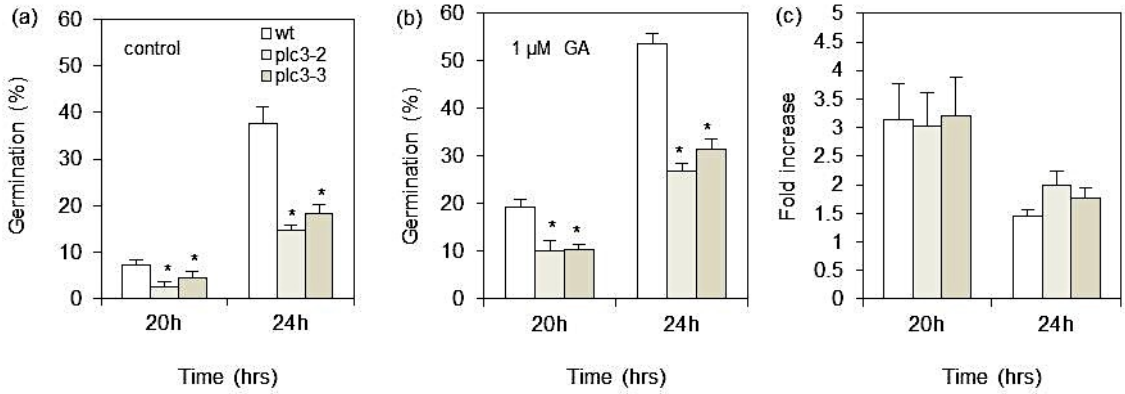

Supplemental Figure S7. Effect of GA on seed germination of wild-type and *plc3* mutants
Seeds germination rate of wild-type and *plc3* mutants in the absence (a) or presence of 1 µM GA (b). Seeds were germinated on ½MS with 0.5% sucrose plates with or without GA at 22 °C after 2 days of stratification at 4 °C. Germination is defined by radical emergence and was scored at the indicated times. In (c), the relative effect of GA on seed germination is calculated. Data shown are the means ± SE of 3 independent experiments (n=55 seeds for each genotype). Asterisks (*) mark that *plc3* value are significantly different from wild-type based on Student's *t-test* (P< 0.05).

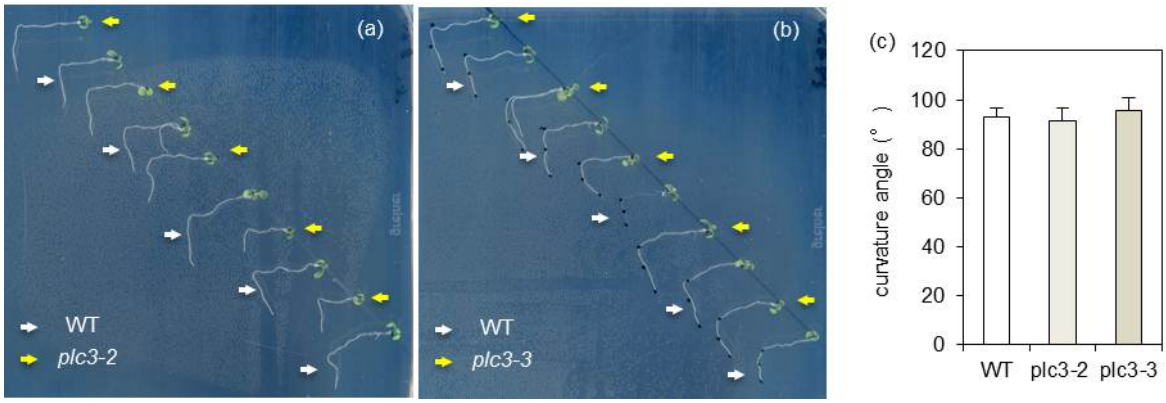

Supplemental Figure S8. Gravitropic response of roots from wild-type and *plc3* mutant seedlings
(a,b) Seedling morphology of wild-type and *plc3* mutants under gravitropic stimulation. Seedlings were grown on ½ MS with 0.5% sucrose plate for 4 days, plates were then rotated by 90°. Photographs were taken 2 days after plate turning (6-d old seedling). (c) Bending was expressed as curvature angle. Values are means ± SD for one representative experiment (n>20). Three independent experiments were performed.